Cell Reports

Article

Beta cells intrinsically sense and limit their secretory activity via mTORC1-RhoA signaling

Graphical abstract

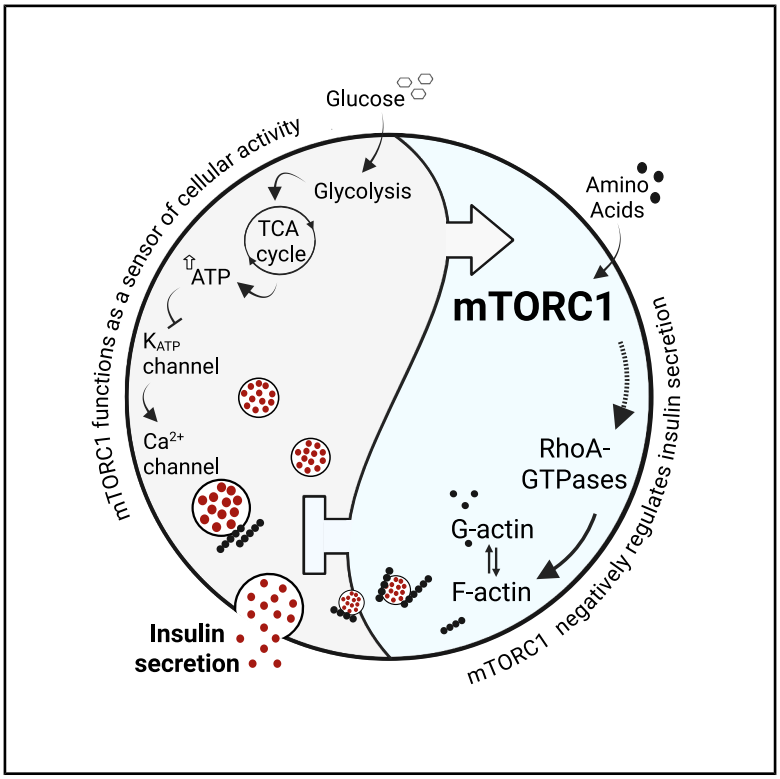

Authors

Saar Krell, Amit Hamburg, Ofer Gover, ..., Kfir Sharabi, Michael D. Walker, Aharon Helman

Correspondence

saarkrell58@gmail.com (S.K.), aharon.helman@mail.huji.ac.il (A.H.)

In brief

Krell et al. show that mTORC1 in β cells acts as an activity sensor, activated by the same signals that trigger insulin secretion. This activation, in turn, inhibits insulin release via RhoA-dependent actin remodeling, establishing a negative feedback loop that allows β cells to intrinsically regulate their own activity.

Highlights

- mTORC1 activation in β cells is coupled to intracellular secretory activity
- Transient mTORC1 inhibition enhances glucose-stimulated insulin secretion
- mTORC1 negatively regulates insulin secretion via RhoA-dependent actin remodeling
- mTORC1 acts as an intrinsic β cell activity sensor and feedback inhibitor

Krell et al., 2025, Cell Reports *44*, 115647
May 27, 2025
https://doi.org/10.1016/j.celrep.2025.115647

CellPress

Cell Reports

CellPress
OPEN ACCESS

Article

Beta cells intrinsically sense and limit their secretory activity via mTORC1-RhoA signaling

Saar Krell,[1,5,*] Amit Hamburg,[1,5] Ofer Gover,[1] Kfir Molakandov,[2] Gil Leibowitz,[3] Kfir Sharabi,[1] Michael D. Walker,[4] and Aharon Helman[1,6,*]

[1]Department of Biochemistry, Food Science and Nutrition, Robert H. Smith Faculty of Agriculture, Food and Environment, Hebrew University of Jerusalem, Rehovot, Israel
[2]Kadimastem Ltd., Weizmann Science Park, Ness Ziona, Israel
[3]Diabetes Unit, Department of Endocrinology and Metabolism, Faculty of Medicine, Hebrew University of Jerusalem, Jerusalem, Israel
[4]Department of Biomolecular Sciences, Weizmann Institute of Science, Rehovot, Israel
[5]These authors contributed equally
[6]Lead contact
*Correspondence: saarkrell58@gmail.com (S.K.), aharon.helman@mail.huji.ac.il (A.H.)
https://doi.org/10.1016/j.celrep.2025.115647

SUMMARY

Precise regulation of insulin secretion by pancreatic β cells is essential to prevent excessive insulin release. Here, we show that the nutrient sensor mechanistic Target of Rapamycin Complex 1 (mTORC1) is rapidly activated by glucose in β cells via the insulin secretion machinery, positioning mTORC1 as a sensor of β cell activity. Acute pharmacological inhibition of mTORC1 during glucose stimulation enhances insulin release, suggesting that mTORC1 acts as an intrinsic feedback regulator that restrains insulin secretion. Phosphoproteomic profiling reveals that mTORC1 modulates the phosphorylation of proteins involved in actin remodeling and vesicle trafficking, with a prominent role in the RhoA-GTPase pathway. Mechanistically, mTORC1 promotes RhoA activation and F-actin polymerization, limiting vesicle movement and dampening the second phase of insulin secretion. These findings identify a glucose–mTORC1–RhoA signaling axis that forms an autonomous feedback loop to constrain insulin exocytosis, providing insight into how β cells prevent excessive insulin release and maintain metabolic balance.

INTRODUCTION

In response to elevated blood glucose levels, pancreatic islet β cells secrete insulin in a biphasic manner.[1–3] Insulin secretion is triggered by glucose metabolism, initiating a cellular cascade that involves the closure of ATP-dependent potassium (K_{ATP}) channels, membrane depolarization, and an increase in cytosolic Ca^{2+} concentration, ultimately leading to a rapid, first-phase exocytosis of a readily releasable pool of insulin granules. Following this initial peak, insulin release is inhibited and drops to 2- to 5-fold above basal secretion. Second-phase insulin secretion requires the recruitment of granules from intracellular storage pools to the plasma membrane and involves the reorganization of the filamentous actin (F-actin) that acts as a barrier for insulin granule release.[4] While the Rho family of GTPases, including Cdc42, Rac, and RhoA, is known to be crucial for second-phase insulin release and F-actin remodeling, the mechanistic regulation of this phase remains poorly understood, particularly the signals linking glucose stimulation to GTPases activation and F-actin dynamics.[5,6]

While potassium chloride (KCl) and other non-nutrient secretagogues can induce the initial, first-phase insulin release, only nutrients can sustain the second-phase release through F-actin remodeling.[7,8] This positive regulation involves not just glucose, but also amino acids, metabolic signals like NADPH, malonyl-CoA, and glutamate, as well as hormones like glucagon-like peptide 1 (GLP-1) and gastric inhibitory polypeptide (GIP).[1,9] Given the critical role of F-actin in mediating this nutrient-driven positive feedback, it is reasonable that signals responsible for negative feedback regulation of insulin secretion might also act through F-actin remodeling. Inhibitory mechanisms are required for tight balance and control of the second-phase insulin secretion. Indeed, there are reports of paracrine-negative regulators, such as somatostatin and epinephrine that transiently repolarize the β cell or raise the threshold for glucose-induced insulin secretion.[3,10–12] However, it is unlikely that paracrine regulation is the sole inhibitory mechanism of the insulin second-phase because the speed of response of β cells to glucose levels around them implies a cell-intrinsic inhibitory mechanism that prevents hyperinsulinemia. Moreover, recent data show that isolated islets composed exclusively of β cells exhibit insulin secretion dynamics similar to that of intact islets, with preserved first and second secretion phases upon glucose stimulation, further implying that β cells intrinsically

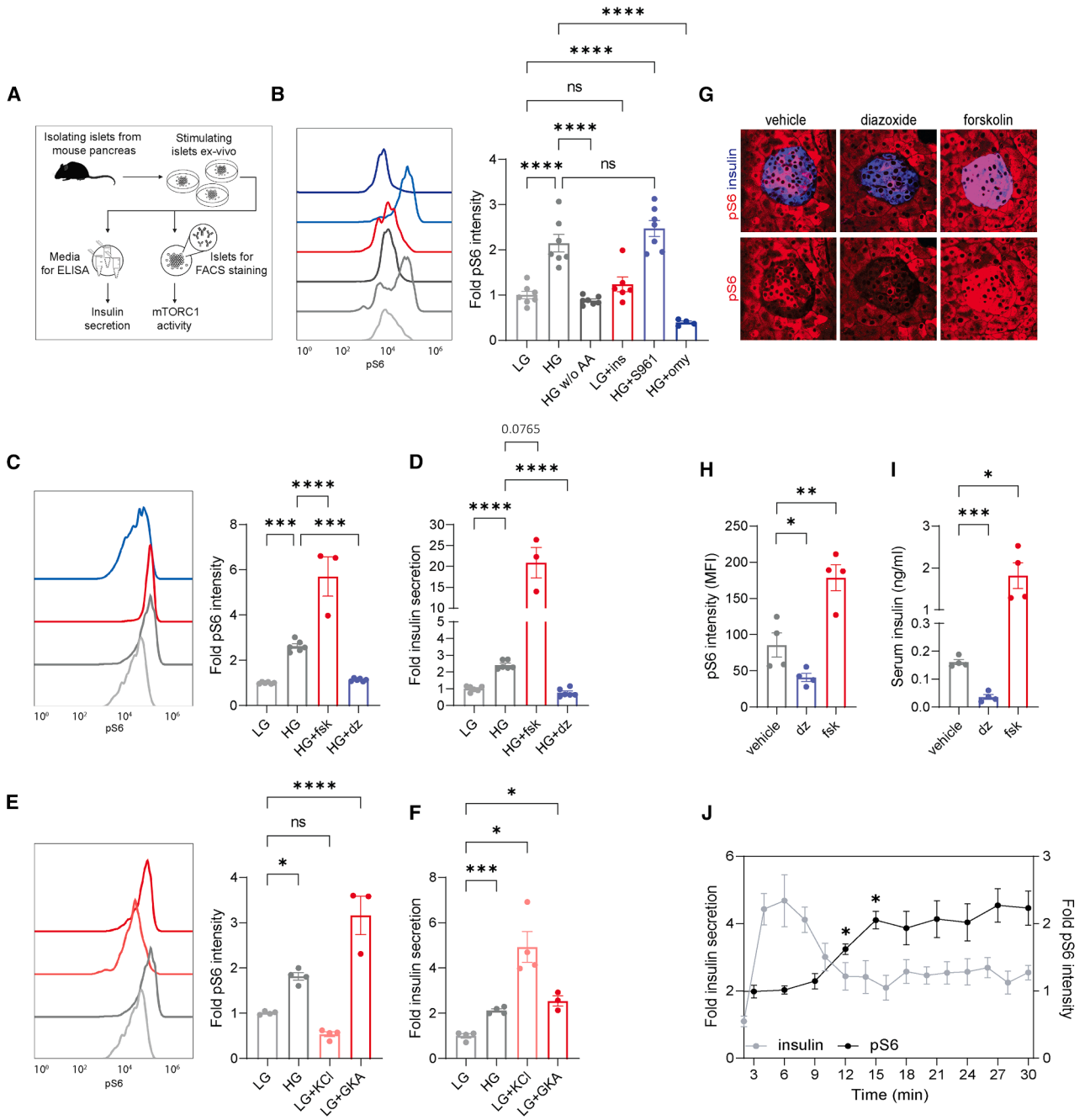

Figure 1. mTORC1 is a β cell secretory sensor

(A) A schematic representation of the experimental method for simultaneous measurement of mTORC1 activity in β cells by FACS and insulin secretion by ELISA.

(B and C) Representative histogram and quantification of pS6 intensity in mouse β cells from isolated islets incubated in RPMI medium with low (LG, 2.8 mM) or high (HG, 16.7 mM) glucose concentrations, and the indicated compounds, for 45 min, as detected by FACS. pS6 intensity is shown relative to the value observed for islets with low glucose (defined as 1). In (B), *n* = 7, 7, 6, 7, and 4 biological replicates, and in (C), *n* = 6, 6, 3, and 6 biological replicates.

(D) Mean insulin levels secreted by mouse islets incubated in RPMI medium with LG or HG and the indicated compounds for 45 min. Secreted insulin levels are shown relative to the value observed for islets with low glucose (defined as 1). *n* = 6, 6, 3, and 6 biological replicates. ins = insulin; S961 = insulin receptor antagonist; omy = oligomycin; fsk = forskolin; dz = diazoxide.

(E and F) Representative histogram and quantification of β cells' pS6 intensity (*n* = 4, 4, 4, and 3 biological replicates) (E) and mean insulin levels secreted by mouse islets (*n* = 4, 4, 4, and 3 biological replicates) (F) incubated in the specified conditions. KCl = potassium chloride; GKA = glucokinase activator.

(legend continued on next page)

control insulin secretion.[13] The lack of evidence for intrinsic negative feedback mechanisms within β cells suggests the potential involvement of other, yet-to-be-discovered, regulatory pathways.

The mechanistic Target of Rapamycin Complex 1 (mTORC1), activated by glucose, amino acids, and growth factors, is essential for the growth, adaptation, and function of pancreatic β cells. It acts as a central signaling hub, integrating both cell-autonomous and systemic growth signals through downstream targets like 4E-BP1, rpS6, and ULK1.[14–20] Studies using genetic gain- and loss-of-function models of mTORC1 pathway components have highlighted its crucial role in β cell physiology,[17,21–27] particularly during fetal development, the early postnatal period, and functional maturation.[28–32] These studies also underscore the importance of tight mTORC1 regulation, as chronic dysregulation, often associated with hyperglycemia, can impair β cell survival, protein synthesis, and autophagy, ultimately impacting insulin secretion and glucose homeostasis.[33,34]

Besides mTORC1, the other mTOR complex, mTORC2, containing the Rapamycin-Insensitive Companion of mTOR (RICTOR), is crucial for maintaining β cell health. Studies in mice lacking RICTOR specifically in β cells have shown a loss of β cell mass, decreased proliferation, reduced insulin content, and abnormal actin polymerization. These defects collectively contribute in a long-term manner to impaired insulin secretion and hyperglycemia.[35–38]

While previous research has focused on the chronic effects of mTORC1 and mTORC2 dysregulation on β cell physiology, its transient effects on β cell function, particularly insulin secretion dynamics, are poorly understood. Here we show that mTORC1 acts as an intracellular sensor of β cell activity, dynamically regulating protein phosphorylation to rapidly control nutrient-stimulated insulin release.

RESULTS

mTORC1 is a cell-autonomous secretory sensor

To simultaneously measure mTORC1 activity and insulin secretion, primary murine islets were stimulated *ex vivo* with glucose in RPMI 1640 medium (RPMI). This medium contains amino acids and vitamins, generally absent in the Krebs Ringer Bicarbonate (KRB) buffer widely used for insulin secretion assays, offering a rich nutrient environment relevant to exploring mTORC1 activity during insulin secretion (Figure 1A).[39,40] While RPMI enables mTORC1 activity (Figure S1A), it generates a weaker insulin secretion response than KRB, both in the first and second phases (Figures S1B and S1C). Following short incubations in RPMI with low and high glucose concentrations (2.8 and 16.7 mM, respectively), media samples were collected for insulin secretion measurement and islets were immediately dispersed and fixed for fluorescence-activated cell sorting (FACS) analysis (Figure 1A). Following a 45-min incubation, mTORC1 activity was strongly induced by high glucose, as demonstrated by increased phosphorylation of ribosomal protein S6 (pS6) (Figure 1B), which correlated with insulin secretion levels (Figure 1D). Concurrently, phosphorylation of 4E-BP1, a direct mTORC1 target, increased in response to glucose (Figure S1J), while phosphorylation of AMPK, an mTORC1 regulator sensitive to ATP levels, decreased (Figure S1K). These observations indicate that the mTORC1 pathway is acutely activated by glucose.

We next examined whether insulin itself directly activates mTORC1 in β cells through a paracrine signaling mechanism involving insulin receptor signaling. Interestingly, unlike glucose, adding external insulin to RPMI containing a low glucose concentration did not increase mTORC1 activity in β cells (Figure 1B). This observation was further supported by the lack of change in pS6 staining upon blocking insulin receptor signaling with the insulin receptor antagonist S961 in RPMI containing high glucose (Figure 1B). These findings suggest that, within the time frame of our experiment, glucose activates mTORC1 in β cells independently of insulin signaling, in agreement with previous reports.[41] Concomitantly, blocking ATP generation using oligomycin effectively abolished pS6 staining (Figure 1B), suggesting that the primary signal activating mTORC1 in β cells is intrinsic rather than paracrine or autocrine.

Given that insulin signaling itself does not appear to be the direct mediator of glucose-dependent mTORC1 activation, we next explored whether other aspects of insulin secretion, such as the secretory pathway, play a role. First, we stimulated insulin secretion at high glucose levels using forskolin (a PKA activator) and exendin-4 (a GLP-1 analog). These drugs enhance insulin release through PKA-mediated calcium influx.[42,43] Increasing insulin secretion through these methods also enhanced mTORC1 activation, as evidenced by increased phosphorylation of S6 and 4E-BP1 (Figures 1C, 1D, S1D, S1E, and S1J).[44] Conversely, inhibiting insulin secretion with diazoxide (an ATP-sensitive potassium channel opener) and nifedipine (a calcium-channel blocker) significantly reduced both insulin secretion and mTORC1 activity, even in the presence of glucose and amino acids (Figures 1C, 1D, S1F, S1G, and S1J).[45] These findings suggest that the secretory machinery in β cells plays a key role in driving mTORC1 activation.

Pharmacologically stimulating insulin secretion in low glucose conditions through membrane potential manipulation (using KCl or the potassium channel blocker tolbutamide) did not activate mTORC1 (Figures 1E, 1F, S1H, and S1I). This suggests that insulin stimulation alone, without glucose and ATP, is insufficient to activate mTORC1. However, using a glucokinase activator (GKA), which increases insulin secretion by directly promoting glucose metabolism, did enhance pS6 staining in low glucose (Figures 1E and 1F). This finding suggests that glucose utilization plays a crucial step in mTORC1 activation.

Next, to validate these findings *in vivo*, we administered glucose with either diazoxide or forskolin to fasted mice.

(G–I) Representative immunostainings of insulin (labeling β cells, blue) and pS6 (red) in pancreatic islets (G) and pS6 intensity quantification in β cells ($n = 4$ mice per group) (H) and serum insulin levels ($n = 4$ mice per group) (I) of wild-type (WT) C57BL per six mice injected with glucose together with the indicated compounds. (J) Comparison of pS6 intensity and dynamic insulin secretion within 30 min of glucose stimulation. Note that pS6 is significantly increased after 12 min and reaches its peak activity after 15 min, by a Student's t test (pS6 [black] $n = 6$ biological replicates, insulin [gray] $n = 4$ biological replicates). Biological replicates represent groups of islets pooled from multiple mice. Data points represent mean ± SEM. $^{*}p < 0.05$, $^{**}p < 0.01$, $^{***}p < 0.005$, $^{****}p < 0.001$.

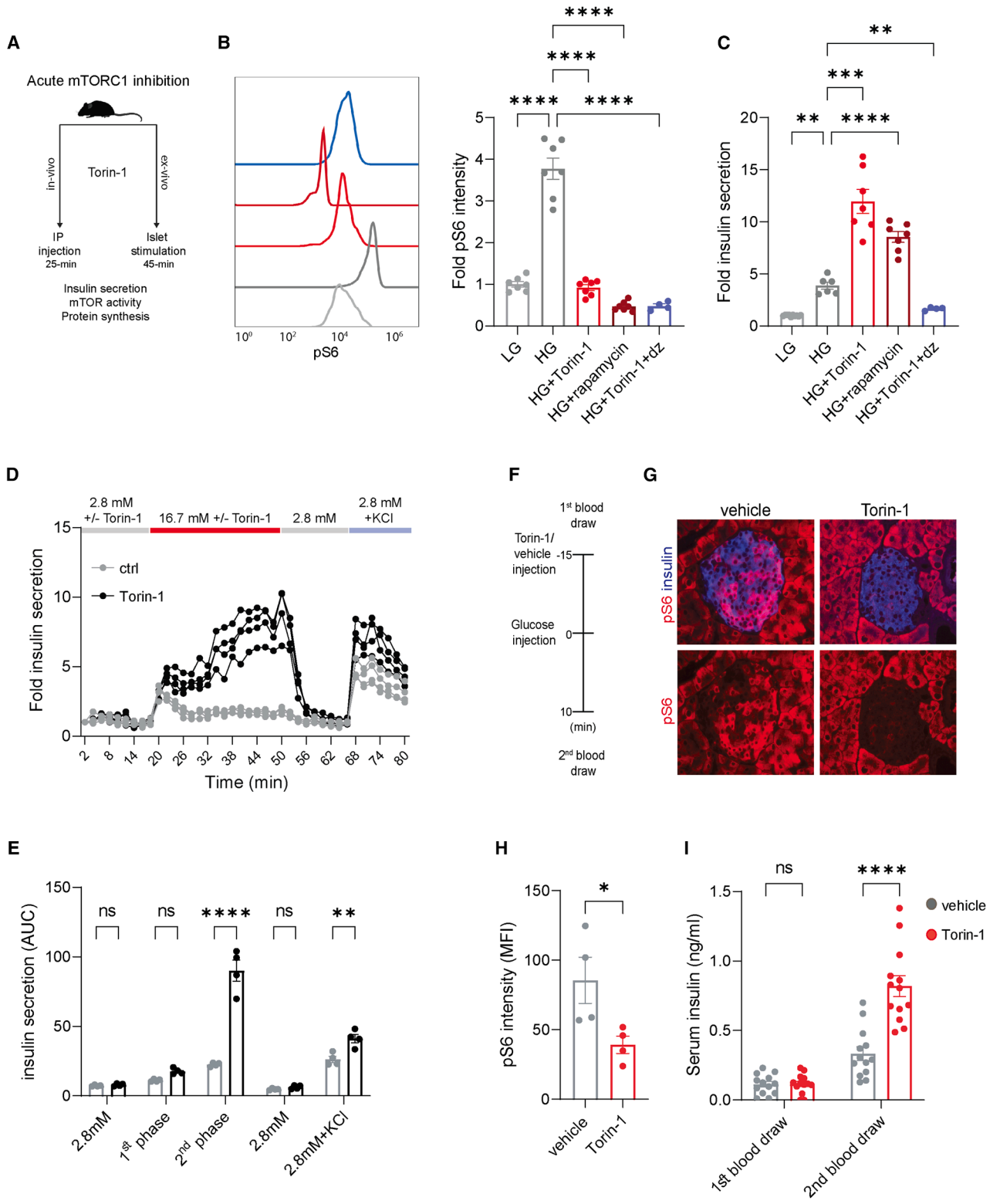

Figure 2. Acute mTORC1 inhibition enhances insulin secretion

(A) A schematic representation of the experimental method for simultaneously measuring mTORC1 activity, protein synthesis, and insulin secretion in mouse β cells.

(legend continued on next page)

Diazoxide-treated mice showed reduced pS6 staining compared with controls, while forskolin significantly increased pS6 staining in β cells, correlating with blood insulin levels (Figures 1G–1I).

Finally, we aimed to understand the dynamics of mTORC1 activation with insulin secretion following glucose stimulation. To investigate this, primary murine islets were incubated *ex vivo* in high glucose for 30 min, with a collection of islet samples every 3 min to enable continuous measurement of mTORC1 activity. Notably, pS6 staining was significantly increased after 15 min while dynamic glucose-stimulated insulin secretion (GSIS) experiments show a faster increase in insulin levels in the media (Figure 1J). Interestingly, mTORC1 activity coincides with the lower second phase of insulin secretion, suggesting a regulatory role in the insulin secretion pathway.

Taken together, these results suggest that mTORC1 activation in β cells requires the activation of the insulin secretory pathway including glucose metabolism, ATP-dependent membrane depolarization, and calcium influx. Importantly, insulin itself or the secretion of insulin in the absence of amino acids or glucose metabolism is not sufficient for mTORC1 activation (Figure 1B). This dependence on β cell activity highlights mTORC1 as an activity sensor.

mTORC1 inhibits insulin secretion in a feedback manner

To investigate whether mTORC1 activity regulates insulin secretion, we acutely inhibited mTORC1 with Torin-1, a potent mTOR inhibitor, during glucose stimulation (Figure 2A). Torin-1 effectively suppressed S6 phosphorylation (Figure 2B). Surprisingly, Torin-1 treatment significantly increased GSIS (Figure 2C). To confirm that this effect was specifically mediated by mTORC1 inhibition, we treated isolated islets with rapamycin, a more specific mTORC1 inhibitor. This specificity was supported by our observation that, while Torin-1 inhibited the glucose-induced Akt S473 phosphorylation (indicative of mTORC2 activation), rapamycin did not, even in higher concentration or longer treatment (Figures S2E and S2F).[46] Acute rapamycin treatment similarly increased GSIS, confirming that this effect is primarily mediated through mTORC1, and not mTORC2, inhibition (Figure 2C). Neither Torin-1 nor rapamycin substantially increased insulin secretion at low glucose levels, indicating that their effect is specific to GSIS and not due to non-specific β cell damage (Figures S2A and S2B). To further ensure that the observed increase in insulin secretion upon mTORC1 inhibition was not simply a result of β cell death and passive insulin release, we co-administered Torin-1 with diazoxide. Pre-treatment with diazoxide completely abolished the Torin-1-induced increase in insulin secretion (Figure 2C). This result strongly suggests a regulated process, wherein mTORC1 inhibition actively enhances insulin release from β cells.

To investigate the effect of Torin-1 on insulin secretion dynamics, we performed a perfusion assay using low (2.8 mM) and high (16.7 mM) glucose concentrations, as well as KCl (30 mM). Torin-1, added during both low and high glucose stimulation, significantly enhanced the second phase of GSIS, while the first phase of GSIS and secretion at low glucose remained unaffected (Figures 2D and 2E). Interestingly, Torin-1 also enhanced KCl-stimulated secretion, without affecting the preceding low glucose phase (Figures 2D and 2E). These results suggest that mTORC1 inhibition primarily affects granule mobilization, possibly through altered actin remodeling, facilitating movement toward the cell membrane. This would primarily impact the second phase of GSIS, which is largely regulated by this process, and also enhance KCl-stimulated secretion, likely due to the relatively close proximity of granules to the cell membrane during this phase.

To examine the temporal dynamics of insulin secretion, we measured its release at 30, 60, and 90 min after glucose stimulation, both with and without Torin-1. While glucose alone elicited a modest increase in insulin secretion, co-treatment with Torin-1 resulted in a significant increase at each time point (Figure S2C). This observation suggests that mTORC1 activity may act as a brake on insulin secretion, preventing a prolonged uncontrolled insulin release.

To determine the specificity of mTORC1 inhibition on insulin secretion, we assessed the impact of Torin-1 on α cell function. mTORC1 inhibition under low glucose conditions led to a significant increase in glucagon secretion (Figure S2D). These findings suggest a broader role for mTORC1 as a general activity sensor and secretion regulator within endocrine cells.[47]

Finally, we validated the physiological relevance of our *ex vivo* observations by examining the effect of acute mTORC1 inhibition on insulin secretion *in vivo*. We injected mice with Torin-1 after overnight fasting and subsequently administered glucose intraperitoneally (scheme, Figure 2F). Blood samples were collected before Torin-1 injection and after glucose administration, allowing us to measure changes in circulating insulin levels (scheme, Figure 2F). Immunostaining of pancreatic islets revealed a specific reduction in pS6 staining in Torin-1-treated mice, confirming effective mTORC1 inhibition (Figures 2G–2I). Strikingly, Torin-1-treated mice exhibited an ∼2.5-fold increase

(B) Representative histogram and quantification of pS6 intensity in mouse β cells from isolated islets incubated in RPMI medium with LG or HG and acute inhibition (45 min) of mTORC1 with Torin-1 or rapamycin, and Torin-1 with diazoxide (dz) (islets were pre-incubated with diazoxide for 30 min). n = 7, 7, 7, 7, and 4 biological replicates.
(C) Mean insulin levels secreted by mouse islets following acute mTORC1 inhibition. Secreted insulin levels are shown relative to the value observed for islets with low glucose (defined as 1). n = 7, 7, 7, 7, and 4 biological replicates. dz = diazoxide.
(D) Fold insulin levels secreted by mouse islets in a representative dynamic perfusion assay in RPMI with LG (±Torin-1), HG (±Torin-1), LG (w/o Torin-1), and KCl (w/o Torin-1). Torin-1 (n = 4 biological replicates, black), control (n = 4 biological replicates, gray).
(E) Area under the curve (AUC) analysis of the dynamic perfusion assay for LG, HG first-phase (18–26 min), HG second-phase (26–54 min), LG, and KCl.
(F) A schematic representation of the experimental method for insulin secretion following acute mTORC1 inhibition, *in vivo*.
(G–I) Representative immunostainings (G) and quantification (H) of pS6 (red) intensity (n = 4 mice per group) in pancreatic β cells (insulin, blue) of fasted mice injected with vehicle or Torin-1, followed by glucose administration. (I) Serum insulin levels of wild-type (WT) C57BL/6 mice before and after intraperitoneal injection of glucose with vehicle or Torin-1. n = 13 mice per group. Biological replicates represent groups of islets pooled from multiple mice. Data points represent mean ± SEM. $^{*}p < 0.05$, $^{**}p < 0.01$, $^{***}p < 0.005$, $^{****}p < 0.001$.

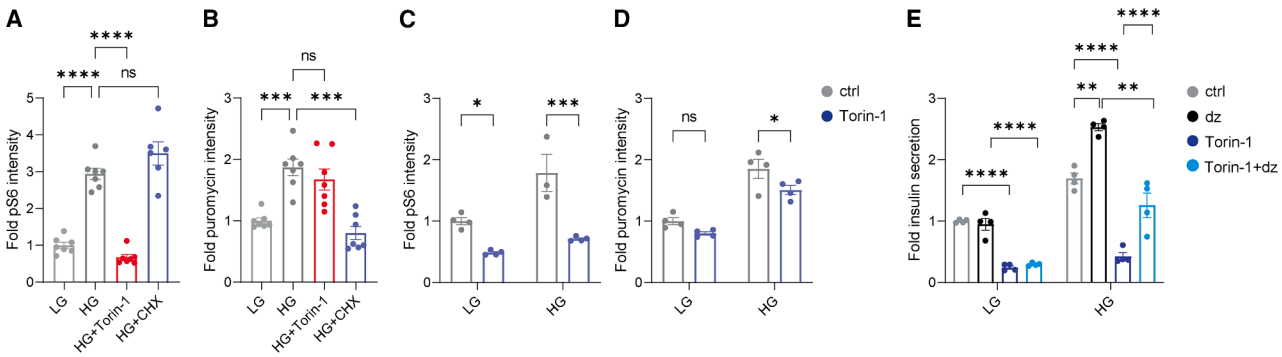

Figure 3. Glucose-mediated protein synthesis is regulated independently of mTORC1

(A and B) Mean pS6 (A) and puromycin (B) intensity, in mouse islets' β cells following acute treatment with Torin-1 and cycloheximide (CHX) during the stimulation with high glucose in RPMI (HG, 16.7 mM). In (A), n = 7, 7, 7, and 6 biological replicates and in (B), n = 7 biological replicates.

(C–E) Mean pS6 (n = 4, 4, 3, and 4 biological replicates) (C), puromycin intensity (n = 4 biological replicates) (D), and fold insulin secreted levels (E) from isolated mouse islets (n = 4 biological replicates), measured after 45 min of incubation in the specified conditions following a 42-h incubation with or without Torin-1 and with or without diazoxide (dz). Biological replicates represent groups of islets pooled from multiple mice. Data points represent mean ± SEM. *p < 0.05, **p < 0.01, ***p < 0.005, ****p < 0.001.

in insulin levels compared with vehicle-injected controls (Figure 2I). These *in vivo* findings are in agreement with the *ex vivo* observations, solidifying the negative association between mTORC1 and insulin secretion.

Glucose-mediated protein synthesis is mTORC1-independent

Intrigued by the unexpected increase in insulin secretion observed upon mTORC1 inhibition, we next examined mTORC1's canonical role in protein synthesis. Using puromycin incorporation as a measure of protein synthesis during glucose stimulation,[48] we observed a significant increase in β cells, which was effectively suppressed by the protein synthesis inhibitor cycloheximide (Figure 3B). Surprisingly, Torin-1 had no significant impact on glucose-stimulated protein synthesis in β cells (Figures 3A and 3B). In contrast, insulin stimulation of primary hepatocytes triggered a significant increase in both mTORC1 activity and protein synthesis, the latter being highly dependent on mTORC1 signaling, as demonstrated by its near-complete inhibition by Torin-1 (Figure S3A). While α and δ cells also displayed reduced protein synthesis upon Torin-1 exposure, the effect was less pronounced compared with cycloheximide treatment (Figures S3B and S3C). Collectively, these findings suggest that while mTORC1 is crucial for protein synthesis in hepatocytes and likely plays a partial role in α and δ cells, β cells utilize an mTORC1-independent pathway for their rapid post-secretory protein synthesis.[49]

We further investigated the long-term effects of mTORC1 inhibition on protein synthesis and GSIS in β cells. A 42-h exposure to Torin-1 robustly suppressed the stimulatory effect of glucose on mTORC1 activity (Figure 3C). This prolonged mTORC1 inhibition resulted in reduced glucose-stimulated protein synthesis and insulin secretion (Figures 3D and 3E), consistent with observations in chronic mTORC1 inhibition mouse models. The effect on GSIS of Torin-1 is partially reversed when the islets are co-incubated with diazoxide, suggesting that part of the effect of β cell dysfunction is due to uncontrolled insulin secretion that leads to β cell exhaustion (Figure 3E). These findings highlight the important role that mTORC1 plays in regulating distinct β cell functions across different time scales to prevent hyperinsulinemia and β cell dysfunction, potentially indicating divergent signaling pathways for immediate and long-term responses to glucose stimulation.

Phosphoproteomics reveals multiple targets affected by acute mTORC1 inhibition in human β cells

To assess the role of mTORC1 in regulating insulin secretion in human β cells, we treated isolated human islets from three independent donors with Torin-1 or rapamycin (Figures 4A and S4A). Both inhibitors markedly increased insulin secretion, mirroring the effects observed in mouse β cells (Figures 4B, 4C, and S4C–S4E). This effect was also observed in human stem-cell-derived islets (SC-islets) from five different differentiation batches (Figure S4F). This conservation of effect across species underscores the importance of mTORC1 regulation in human β cell function.

To elucidate the mechanism by which mTORC1 inhibition affects insulin secretion, we investigated the immediate impacts of mTORC1 kinase activity on protein phosphorylation. Glucose-responsive human islets (validated by GSIS assays in both KRB and RPMI media; Figures S4B and S4C–S4E) were stimulated with glucose for 45 min, with or without rapamycin. In parallel, SC-islets were stimulated with glucose for 45 min, with or without Torin-1. Phosphoproteomic analysis of these experiments revealed that acute mTORC1 inhibition in both human primary islets and SC-islets affected multiple pathways, including those of the mTORC1 pathway, membrane trafficking, and pancreatic β cell function (Figures 4D and S4G and Table S1). In addition to known downstream mTORC1 targets such as ribosomal protein S6 kinase (RPS6K) and eukaryotic translation initiation factors (eIF4), several β cell-specific factors, including MLXIPL, NKX2, and RFX6, were also found to be targeted by mTORC1 (Figures 4E and S4H). Pathway enrichment analysis (Enrichr) revealed that the most significantly affected pathway, besides the mTOR signaling pathway, was the RhoA-GTPase pathway[59,60] (Figures 4D and S4G). This pathway, involved in actin

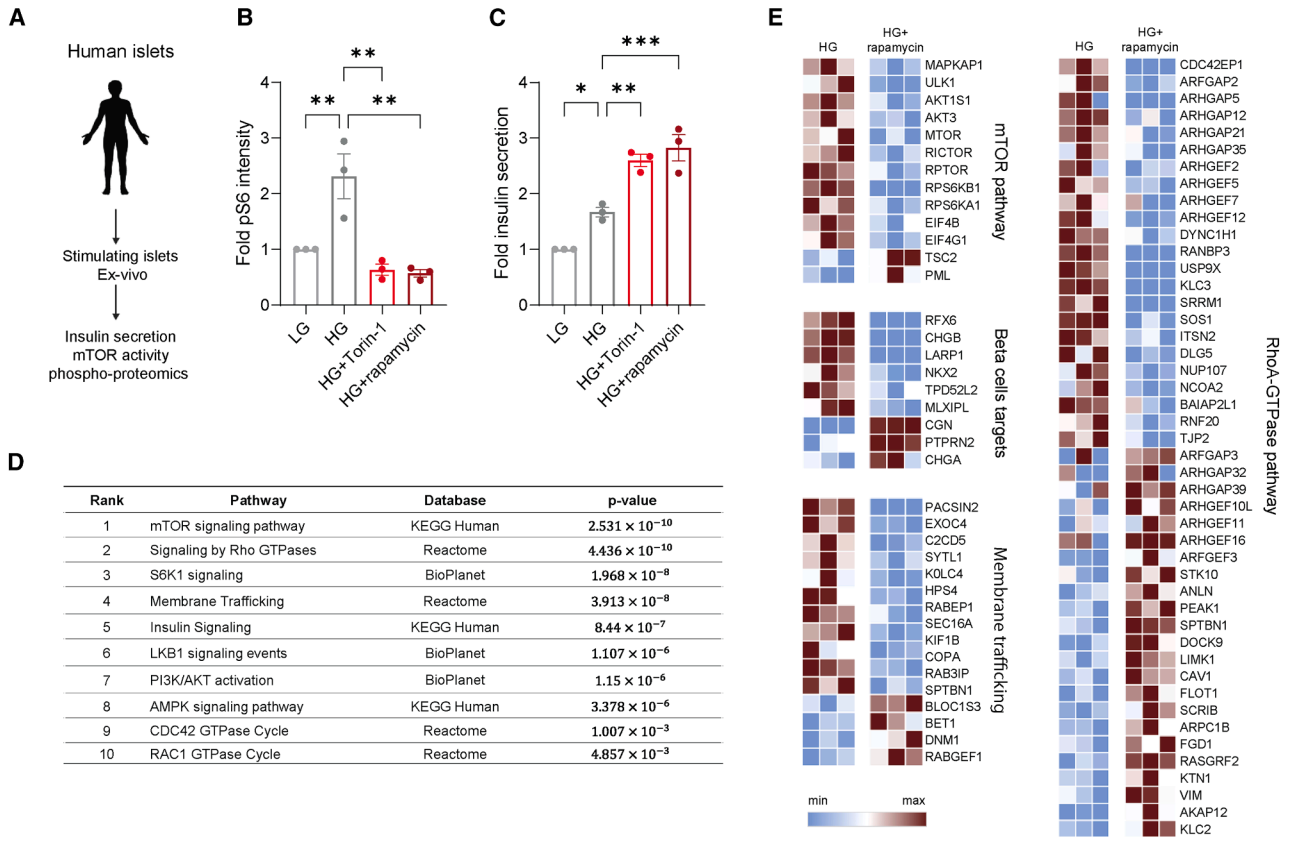

D

Rank	Pathway	Database	p-value
1	mTOR signaling pathway	KEGG Human	2.531×10^{-10}
2	Signaling by Rho GTPases	Reactome	4.436×10^{-10}
3	S6K1 signaling	BioPlanet	1.968×10^{-8}
4	Membrane Trafficking	Reactome	3.913×10^{-8}
5	Insulin Signaling	KEGG Human	8.44×10^{-7}
6	LKB1 signaling events	BioPlanet	1.107×10^{-6}
7	PI3K/AKT activation	BioPlanet	1.15×10^{-6}
8	AMPK signaling pathway	KEGG Human	3.378×10^{-6}
9	CDC42 GTPase Cycle	Reactome	1.007×10^{-3}
10	RAC1 GTPase Cycle	Reactome	4.857×10^{-3}

Figure 4. mTORC1 phosphorylates multiple functional targets and regulates insulin secretion in human β cells

(A) A schematic representation of the experimental method for simultaneously measuring mTORC1 activity, quantifying insulin secretion, and characterizing the phospho-proteome in cadaveric human islets.

(B and C) Mean pS6 intensity and insulin secretion levels by human cadaveric islets following LG and HG stimulation with acute mTORC1 inhibition using Torin-1 or rapamycin. $n = 3$ human donors (#1–3 in Figure S4). Data points represent mean ± SEM. $^{*}p < 0.05$, $^{**}p < 0.01$, $^{***}p < 0.005$, $^{****}p < 0.001$.

(D) Main pathways from a gene set enrichment analysis of the differentially phosphorylated proteins following acute rapamycin treatment.

(E) Heatmaps of the phosphorylation levels of selected proteins affected by mTORC1 inhibition as analyzed by phosphoproteomics assay and plotted by Morpheus ($n = 3$ technical replicates of human donor #4 in Figure S4).[50–58]

polymerization and known to regulate insulin secretion (scheme, Figure 5A), showed alterations in multiple proteins controlling RhoA activation, including ARFGAP, ARHGAP, and ARHGEF proteins, suggesting mTORC1-mediated regulation of RhoA-GTPase downstream of glucose stimulation (Figures 4E and S4H).[61–63]

mTORC1 controls actin remodeling via RhoA activation

To determine if the observed phosphoproteomic changes in key members of the RhoA signaling pathway reflected alterations in RhoA activity, we examined the phosphorylation levels of its downstream effector, MLC2 (Figure 5A).[64,65] FACS analysis showed decreased MLC2 phosphorylation in both mouse and human β cells following acute mTORC1 inhibition (Figures 5B and S5A). In mouse islets, this reduction in pMLC2 due to mTORC1 inhibition resembled the effect of ML-7, an MLC kinase inhibitor (Figure S5A). These findings suggest that mTORC1, directly or indirectly, regulates RhoA-GTPase activity. Consistent with RhoA's role in actin remodeling, F-actin levels were significantly reduced in β cells treated with Torin-1 or rapamycin, as demonstrated by F-actin antibody and phalloidin staining (Figures 5C and S5B). Latrunculin A, a known actin polymerization inhibitor, was used as a positive control to validate the specificity of phalloidin.[66–69] Pharmacological RhoA inhibition, using rhosin, also yielded similar reductions in actin polymerization (Figure 5C).[70] To confirm that the ratio of F- to G-actin changes following acute treatment with Torin-1, we performed an F/G-actin ratio assay, which revealed an increase in G-actin concomitant with decreased F-actin levels (Figure 5D), facilitating insulin granule movement and exocytosis. Consistently, phalloidin staining of pancreatic islets following *ex vivo* mTORC1 inhibition with rapamycin showed decreased levels compared with high glucose alone (Figure 5E). Consistent with these findings, immunostaining of pancreatic slices showed that acute Torin-1 administration also resulted in a marked reduction in cortical F-actin, as visualized by co-staining with E-cadherin, a marker of the cortical membrane (Figure 5F and Video S1).[71]

Given that RhoA is known to influence calcium ion influx,[72] we investigated the effect of mTORC1 inhibition on calcium influx by using the genetically encoded calcium indicator GCaMP8m, expressed via adeno-associated virus (AAV) in isolated mouse

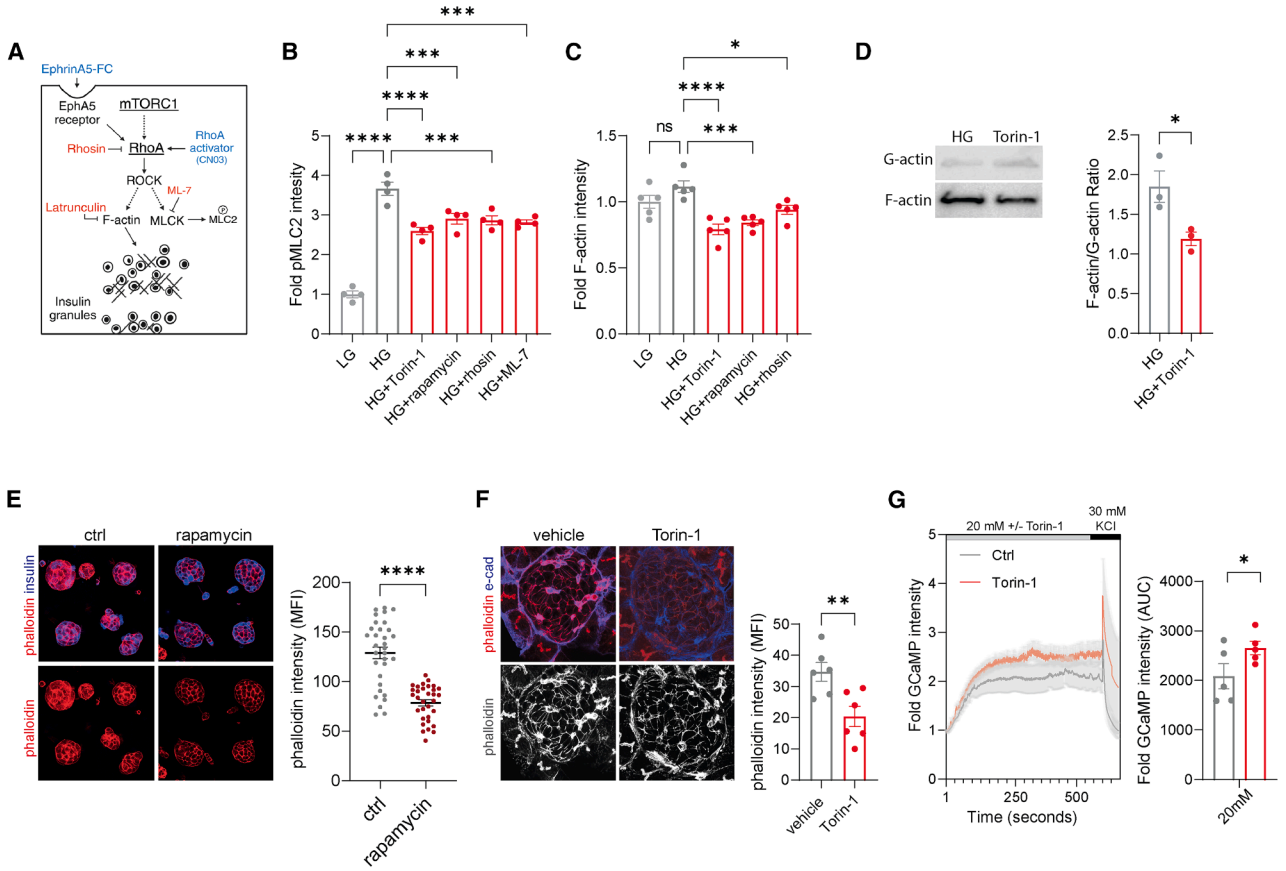

Figure 5. mTORC1 activates RhoA and controls actin polymerization

(A) A scheme showing the mechanism in which RhoA-GTPase remodels F-actin to control insulin secretion.

(B and C) Mean pMLC2 (n = 4 biological replicates) (B) and F-actin intensity (determined by anti-F-actin, ab205) (n = 5 biological replicates) (C) in mouse islets following incubation in RPMI with the specified treatments for 45 min rhosin (RhoA inhibitor), ML-7 (MLCK inhibitor).

(D) Immunoblot analysis and quantification of Torin-1-induced changes in soluble (G-actin) and insoluble (F-actin) fractions in mouse islets treated with 16.7 mM glucose (HG), with or without Torin-1, for 45 min.

(E) Representative immunostainings and quantification of phalloidin (red) intensity in pancreatic β cells (insulin, blue) of isolated islets incubated in RPMI with or without rapamycin. n = 32 islets for each treatment, derived from three independent experiments.

(F) Representative immunostainings and quantification of phalloidin (red) intensity in fasted mice injected with glucose and vehicle or Torin-1. Cell cortical membrane detected by E-cadherin (blue) staining. n = 6 mice per group.

(G) Quantification of GCaMP fluorescence intensity in isolated mouse islets infected with AAV.KP1-CAG-GCaMP8m. Islets were stimulated with 20 mM glucose with or without Torin-1, followed by 30 mM KCl for 2 min (n = 5 biological replicates for each treatment). Biological replicates represent groups of islets pooled from multiple mice. Data points represent mean ± SEM. *p < 0.05, **p < 0.01, ***p < 0.005, ****p < 0.001.

islets. Intriguingly, we observed increased calcium influx and oscillations upon Torin-1 inhibition in response to glucose stimulation (Figure 5G and Video S2), consistent with the observed complex effects of mTORC1-RhoA signaling.

mTORC1 controls insulin secretion via RhoA-dependent actin remodeling

To further investigate the connection between mTORC1 activity, actin remodeling, and insulin secretion, we tested the impact of acutely increasing basal mTORC1 activity prior to glucose stimulation. We pre-incubated mouse islets with MHY1485, a small-molecule activator of mTOR, in low-glucose (2.8 mM) media containing amino acids to stimulate mTORC1 activity.[73] S6 phosphorylation confirmed increased mTORC1 activation at the end of the pre-incubation period (Figure 6A). Islets were then stimulated with high glucose for 10 and 45 min to assess the impact on insulin secretion. As shown in Figures 6B–6D, the increased basal mTORC1 activity, induced by MHY1485 pre-treatment, led to increased actin polymerization and reduced insulin secretion after 10 min, which is associated with first-phase insulin secretion. This observation further supports the inhibitory role of mTORC1 in insulin release through actin remodeling, demonstrating that acutely elevating mTORC1 activity prior to glucose stimulation can impair the initial insulin response. Interestingly, after 45 min of glucose stimulation, pS6 levels, actin polymerization, and insulin secretion in the MHY1485 pre-treated group returned to levels comparable to the control group (Figures 6B–6D). This suggests that β cells can dynamically adjust their mTORC1 activity and actin cytoskeleton to modulate insulin secretion and maintain

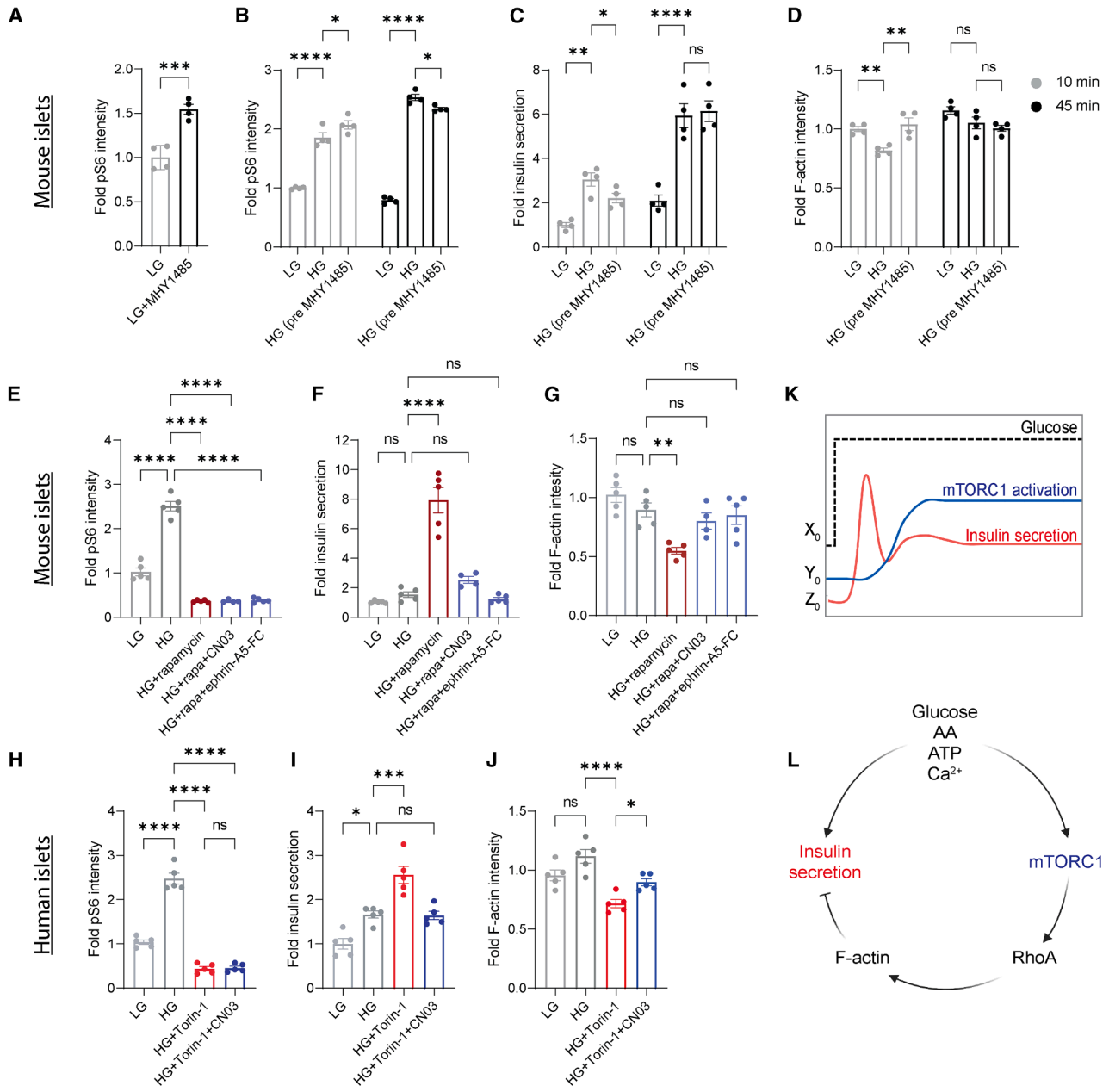

Figure 6. Insulin secretion regulation by mTORC1 is mediated through RhoA-dependent actin polymerization

(A) Mean pS6 intensity in mouse islets' β cells following incubation in RPMI supplemented with 2.8 mM (LG) glucose with or without mTOR activator (MHY1485) for 30 min, *n* = 4 biological replicates.

(B–D) Mean pS6 intensity (B), fold insulin secretion (C), and F-actin intensity (determined by anti-F-actin antibody, ab205) (D) in mouse islets (*n* = 4 biological replicates) were measured after 10 min or 45 min following incubation in RPMI with the indicated treatments.

(E–J) Mouse islets (E–G) and (H–J) human islets were incubated in RPMI with the indicated treatments. Mean pS6 intensity (E and H), insulin secretion (F and I), and F-actin intensity (determined by using mouse anti-F-actin antibody, ab205) (G and J) were measured. Islets treated with the RhoA activator (CN03) or ephrin-A5 FC were pre-incubated for 30 min with each compound. For mouse islets (E–G), *n* = 5, 5, 5, 4, and 5 biological replicates for the respective treatments. For human islets (H–J), *n* = 5 technical replicates of human donor #4 in Figure S4. Biological replicates represent groups of islets pooled from multiple mice. Data are mean ± SEM. *$p < 0.05$, **$p < 0.01$, ***$p < 0.005$, ****$p < 0.001$.

(K) A scheme describing the dynamics of mTORC1-RhoA signaling (Y) and insulin secretion (Z) in response to glucose (X).

(L) A proposed model of the incoherent feedforward negative regulation of insulin secretion by mTORC1 via RhoA-dependent F-actin polymerization in normal conditions.

appropriate secretory output in response to their intrinsic workload.

To confirm that mTORC1 regulates insulin secretion via RhoA, we combined mTORC1 inhibition using rapamycin or Torin-1 with direct pharmacological RhoA activation via CN03.[74] While RhoA activation alone did not inhibit insulin secretion, it significantly attenuated the increased insulin secretion induced by mTORC1 inhibition in both mouse and human islets. (Figures 6E, 6F, 6H, 6I, S6D, and S6E), suggesting that mTORC1's inhibitory effect on insulin secretion is mediated through RhoA. Furthermore, RhoA activation counteracted the reduction in F-actin polymerization caused by mTORC1 inhibition (Figures 6G, 6J, and S6F), indicating that mTORC1 regulates actin dynamics through RhoA, potentially affecting insulin granule trafficking and release. CN03's effects were also apparent with ephrin-A5-FC, which affects insulin secretion in several mechanisms including actin polymerization, as demonstrated by its independent effect on insulin secretion (Figure S6B).[75] Since neither compound increased MLC2 phosphorylation or actin levels alone (Figures S6A and S6C), this may indicate that, under high glucose conditions, induced mTORC1 activity leads to maximal RhoA-mediated actin polymerization, thus limiting insulin secretion. However, following mTORC1 inhibition, which disrupts actin structure, RhoA activation can restore actin polymerization. Taken together, these findings strongly indicate that mTORC1 inhibits insulin secretion by activating the RhoA-GTPase pathway and promoting actin polymerization, thus revealing a critical regulatory mechanism linking nutrient and activity sensing to the intrinsic control of insulin release.

DISCUSSION

Biological processes are often controlled by complex networks with many interacting components. It is therefore expected that a crucial process like insulin secretion would be tightly regulated by both positive and negative feedback loops. One such regulatory system is the incoherent feedforward loop (IFFL), where an input factor (X) regulates both an intermediate factor (Y) and an output (Z), but in opposite directions.[76] Our study reveals that β cells regulate insulin secretion through an IFFL, where glucose (X) positively regulates both insulin secretion (Z) and mTORC1 activity (Y), which in turn negatively regulates insulin secretion (Figures 6K and 6L). IFFLs are known to play diverse roles in biological systems, including generating pulses, accelerating responses, or achieving perfect adaptation—all critical features for a complex system like β cells controlling insulin secretion to achieve glucose homeostasis.[77]

As a critical signaling hub, mTORC1 senses diverse signals, including growth factors, amino acids, stress, oxygen, and energy levels. When activated, mTORC1 promotes protein and lipid synthesis while inhibiting autophagy, thereby controlling cell growth and metabolism.[78] Our study reveals that mTORC1 also senses the cellular activity of β cells, as the same processes that stimulate insulin secretion-glucose metabolism, membrane depolarization, and calcium influx are also required for mTORC1 activation. While calcium's role in mTORC1 activation has been previously noted, its exact mechanism remains to be elucidated.[79,80] Given that membrane depolarization and calcium have critical roles in the function of various cell types, including neurons and muscle cells, we suggest that mTORC1 might have a broader role in sensing and regulating cellular activity beyond its well-established functions in growth and metabolism.[81]

Our research focuses on the immediate, transient impact of mTORC1 activation on β cell activity. We utilize pharmacological inhibitors, such as Torin-1 and rapamycin, to achieve acute and temporary mTORC1 inhibition. Our results reveal a previously unappreciated level of insulin secretion regulation. Unlike other regulatory mechanisms involving paracrine or external stimuli, such as glucose itself or hormones like somatostatin, this mechanism is entirely intrinsic, enabling each β cell to precisely control its individual secretion output. This intrinsic control is significant because it is both precise and immediate; the degree and rate of inhibition are proportional to the cell's workload. While other signals, such as glucose, more dominantly contribute to the regulation of insulin secretion, the intrinsic nature of the mTORC1-mediated pathway provides a crucial layer of cell-autonomous control. This intrinsic regulation may be particularly important in situations where systemic signals are insufficient or delayed, allowing individual β cells to rapidly adjust their secretory output in response to local metabolic cues. Comparing and contrasting the relative contributions of intrinsic and extrinsic regulatory mechanisms will be an important area for future research.

This intrinsic regulatory mechanism may be crucial at the β cell level to prevent exhaustion caused by hypersecretion. Our experiments demonstrate that, in the absence of mTORC1 activity, β cells continue to secrete insulin in an uncontrolled manner. Prolonged hypersecretion, in turn, impairs the cells' ability to respond appropriately to subsequent glucose challenges. At the whole-body level, this mechanism plays a vital role in controlling the second, more sustained phase of insulin secretion that follows the initial burst triggered by glucose stimulation. Precise control of this second phase allows for better adaptation to fluctuating carbohydrate levels, which can vary significantly depending on meal composition. This tight regulation ensures that potent insulin is not over-secreted, thus preventing potentially life-threatening hypoglycemia.

Our findings contrast with those of most previous studies examining the role of mTORC1 in β cells, which have relied on mouse genetic models or extended treatments with mTORC1 inhibitors and typically observe an inhibitory effect of mTORC1 activation on insulin secretion.[33] Even short-term genetic manipulations in mice require at least a few days to manifest, making them effectively "chronic" compared with the acute, transient pharmacological inhibition employed in our study. Specifically, we examined the immediate impact of mTORC1 inhibition during a 45-min *ex vivo* glucose stimulation or following a single intraperitoneal glucose injection. It is important to note that, in our own experiments, prolonged Torin-1 treatment also led to reduced GSIS, likely due to decreased protein synthesis and β cell exhaustion resulting from sustained hypersecretion. This difference in experimental design—acute vs. chronic—may explain why previous studies, using genetic models or prolonged inhibitor treatments, primarily identified extended or indirect effects of mTORC1 on insulin secretion (mediated through proliferation,

protein synthesis, gene expression, and potentially an initial phase of hypersecretion) rather than its direct, immediate role in the insulin secretion pathway itself, as revealed by our current work.

This study establishes a foundation for understanding the complex signaling networks that govern β cell function and dysfunction, particularly in the context of type 2 diabetes (T2D), where mTORC1 activity is known to be dysregulated.[33,82–84] Our findings suggest that mTORC1 acts as a critical rheostat in β cells, precisely balancing insulin secretion with cellular metabolic needs. Insufficient mTORC1 signaling, as observed in our acute inhibition studies, can lead to hyperinsulinemia, potentially contributing to insulin resistance and eventually β cell exhaustion. Conversely, excessive mTORC1 activity, perhaps due to chronic nutrient oversupply or other metabolic stressors, can paradoxically impair insulin release, potentially through the mechanisms we have described, such as altered actin dynamics and impaired vesicle trafficking (Figures 6K and 6L). This impairment could contribute to the progressive decline in β cell function characteristic of T2D. Indeed, the chronic hyperinsulinemia often seen in pre-diabetes and early T2D could be a consequence of the β cell attempting to compensate for this impaired release, further exacerbating the problem. Understanding how these opposing effects of mTORC1 dysregulation contribute to the pathogenesis of T2D is crucial. For example, identifying specific upstream regulators of mTORC1 in β cells could offer therapeutic targets. Similarly, interventions aimed at restoring proper mTORC1 signaling balance—perhaps by selectively modulating its activity or by targeting downstream effectors like the actin cytoskeleton—may prove beneficial in preserving β cell function, delaying the progression to diabetes, and ultimately preventing diabetes-related complications. Further research into these mechanisms holds significant promise for the development of therapeutic strategies to restore β cell function and improve glycemic control in individuals with, or at risk for, T2D.

Limitations of the study

This study focused on the transient effects of mTORC1 activity, necessitating the use of pharmacological inhibitors like Torin-1 and rapamycin. While these inhibitors offer valuable insights into acute mTORC1 modulation, the possibility of off-target effects remains a concern, even though we validated the specificity of rapamycin and Torin-1 to their targets and confirmed their specific effect on insulin secretion, consistent with numerous prior studies. Genetic manipulations, due to their chronic nature, were not suitable for this investigation, as they would not allow us to examine the dynamic changes in signaling pathways and cellular processes associated with acute mTORC1 inhibition.

While human data were generated using scarce and often variably functional human islets, we addressed this limitation by using samples from four donors with technical replicates, the results of which mirrored our findings in mouse islets. Although the limited sample size of human islets could potentially restrict the generalizability of our findings, the consistent results across replicates and species strengthen the overall conclusions of the study. To further support our findings in human β cells, we used SC-islets. Despite their typically low glucose responsiveness, SC-islets exhibited increased insulin secretion with mTORC1 inhibition, consistent with our model. This suggests that aberrant nutrient sensing, leading to high mTORC1 activity, may contribute to SC-β cell dysfunction through our proposed mechanism.[31]

Finally, while our study elucidates a mechanism by which mTORC1 regulates insulin secretion, further research is needed to fully explore the molecular details of how mTORC1, and perhaps mTORC2, regulate insulin secretion dynamics and other β cell activities beyond the RhoA-GTPase pathway and its interaction with the actin cytoskeleton.

RESOURCE AVAILABILITY

Lead contact

Further information and requests for resources and reagents should be directed to and will be fulfilled by the lead contact, Aharon Helman (aharon.helman@mail.huji.ac.il).

Materials availability

This study did not generate new unique reagents.

Data and code availability

Phosphoproteomic data generated in this study have been deposited to PRIDE: PXD062389.

Any additional information required to reanalyze the data reported in this paper is available from the lead contact upon request.

ACKNOWLEDGMENTS

We thank Omer Cohenstam for his technical assistance. We also thank Maya Sherman from The Edmond and Lily Safra Center for Brain Sciences (ELSC) for manufacturing the rAAV vector; Meital Kupervaser from the De Botton Protein Profiling Institute of the Nancy and Stephen Grand Israel National Center for Personalized Medicine, Weizmann Institute of Science, for phosphoproteomics operation and data analysis; Ben Glazer and Dana Avrahami for assistance with the perifusion insulin secretion assay; and Yuval Dor, Agnes Klochendler, and Yael Riahi for helpful discussions. This research was generously supported by grants from the Israel Science Foundation (ISF; grant 1282/21) and Breakthrough Diabetes (grant 1-SRA-2023-1350-A-N).

AUTHOR CONTRIBUTIONS

Conceptualization, A. Helman and S.K.; methodology, S.K. and A. Hamburg; investigation, S.K. and A. Hamburg; writing – original draft, S.K. and A. Helman; writing – review & editing, A. Hamurg, K.S., K.M., G.L., and M.D.W.; funding acquisition, A. Helman and M.D.W.; resources, K.M. and K.S.; supervision, A. Helman.

DECLARATION OF INTERESTS

The authors declare no competing interests.

STAR★METHODS

Detailed methods are provided in the online version of this paper and include the following:

- KEY RESOURCES TABLE
- EXPERIMENTAL MODEL AND STUDY PARTICIPANT DETAILS
  - Mice
  - Human islets
  - Human SC-islets
- METHOD DETAILS

SUPPLEMENTAL INFORMATION

Supplemental information can be found online at https://doi.org/10.1016/j.celrep.2025.115647.

Received: October 10, 2024
Revised: February 24, 2025
Accepted: April 11, 2025

REFERENCES

1. Campbell, J.E., and Newgard, C.B. (2021). Mechanisms controlling pancreatic islet cell function in insulin secretion. Nat. Rev. Mol. Cell Biol. *22*, 142–158. https://doi.org/10.1038/S41580-020-00317-7.
2. Komatsu, M., Takei, M., Ishii, H., and Sato, Y. (2013). Glucose-stimulated insulin secretion: A newer perspective. J. Diabetes Investig. *4*, 511–516. https://doi.org/10.1111/JDI.12094.
3. Rorsman, P., and Ashcroft, F.M. (2018). Pancreatic β-cell electrical activity and insulin secretion: Of mice and men. Physiol. Rev. *98*, 117–214. https://doi.org/10.1152/physrev.00008.2017.
4. Arous, C., and Halban, P.A. (2015). The skeleton in the closet: Actin cytoskeletal remodeling in β-cell function. Am. J. Physiol. Endocrinol. Metabol. *309*, E611–E620. https://doi.org/10.1152/ajpendo.00268.2015.
5. Wang, Z., and Thurmond, D.C. (2009). Mechanisms of biphasic insulin-granule exocytosis - Roles of the cytoskeleton, small GTPases and SNARE proteins. J. Cell Sci. *122*, 893–903. https://doi.org/10.1242/jcs.034355.
6. Kalwat, M.A., and Thurmond, D.C. (2013). Signaling mechanisms of glucose-induced F-actin remodeling in pancreatic islet β cells. Exp. Mol. Med. *45*, e37. https://doi.org/10.1038/EMM.2013.73.
7. Ort, T., Voronov, S., Guo, J., Zawalich, K., Froehner, S.C., Zawalich, W., and Solimena, M. (2001). Dephosphorylation of β2-syntrophin and Ca2+/μ-calpain-mediated cleavage of ICA512 upon stimulation of insulin secretion. EMBO J. *20*, 4013–4023. https://doi.org/10.1093/emboj/20.15.4013.
8. Kalwat, M.A., Yoder, S.M., Wang, Z., and Thurmond, D.C. (2013). A p21-activated kinase (PAK1) signaling cascade coordinately regulates F-actin remodeling and insulin granule exocytosis in pancreatic β cells. Biochem. Pharmacol. *85*, 808–816. https://doi.org/10.1016/j.bcp.2012.12.003.
9. Mann, E., Sunni, M., and Bellin, M.D. (2020). Secretion of Insulin in Response to Diet and Hormones. Pancreapedia: The Exocrine Pancreas Knowledge Base. https://doi.org/10.3998/PANC.2020.16.
10. Huising, M.O. (2020). Paracrine regulation of insulin secretion. Diabetologia *63*, 2057–2063. https://doi.org/10.1007/S00125-020-05213-5.
11. Rorsman, P., and Huising, M.O. (2018). The somatostatin-secreting pancreatic δ-cell in health and disease. Nat. Rev. Endocrinol. *14*, 404–414. https://doi.org/10.1038/S41574-018-0020-6.
12. Peng, X., Ren, H., Yang, L., Tong, S., Zhou, R., Long, H., Wu, Y., Wang, L., Wu, Y., Zhang, Y., et al. (2024). Readily releasable β cells with tight Ca2+–exocytosis coupling dictate biphasic glucose-stimulated insulin secretion. Nat. Metab. *6*, 238–253. https://doi.org/10.1038/s42255-023-00962-0.
13. Perez-Frances, M., Bru-Tari, E., Cohrs, C., Abate, M.V., Léon, van G., Kenichiro, F., Stephan Speier, F.T., and P, L.H. (2024). Regulated and adaptive in vivo insulin secretion from islets only containing β-cells. Nat. Metab. *6*, 1791–1806.
14. Kim, J., and Guan, K.L. (2019). mTOR as a central hub of nutrient signalling and cell growth. Nat. Cell Biol. *21*, 63–71. https://doi.org/10.1038/s41556-018-0205-1.
15. Kim, S.G., Buel, G.R., and Blenis, J. (2013). Nutrient regulation of the mTOR complex 1 signaling pathway. Mol. Cells *35*, 463–473. https://doi.org/10.1007/s10059-013-0138-2.
16. Howell, J.J., and Manning, B.D. (2011). MTOR couples cellular nutrient sensing to organismal metabolic homeostasis. Trends in Endocrinology \& Metabolism *22*, 94–102. https://doi.org/10.1016/j.tem.2010.12.003.
17. Valvezan, A.J., and Manning, B.D. (2019). Molecular logic of mTORC1 signalling as a metabolic rheostat. Nature metabolism *1*, 321–333. https://doi.org/10.1038/s42255-019-0038-7.
18. Condon, K.J., and Sabatini, D.M. (2019). Nutrient regulation of mTORC1 at a glance. J. Cell Sci. *132*, jcs222570. https://doi.org/10.1242/JCS.222570.
19. Liu, G.Y., and Sabatini, D.M. (2020). mTOR at the nexus of nutrition, growth, ageing and disease. Nature reviews Molecular cell biology *21*, 183–203. https://doi.org/10.1038/s41580-019-0199-y.
20. Saxton, R.A., and Sabatini, D.M. (2017). mTOR Signaling in Growth, Metabolism, and Disease. Cell *168*, 960–976. https://doi.org/10.1016/j.cell.2017.02.004.
21. Israeli, T., Riahi, Y., Garzon, P., Louzada, R.A., Werneck-De-castro, J.P., Blandino-Rosano, M., Yeroslaviz-Stolper, R., Kadosh, L., Tornovsky-Babeay, S., Hacker, G., et al. (2022). Nutrient Sensor mTORC1 Regulates Insulin Secretion by Modulating β-Cell Autophagy. Diabetes *71*, 453–469. https://doi.org/10.2337/DB21-0281.
22. Blandino-Rosano, M., Chen, A.Y., Scheys, J.O., Alejandro, E.U., Gould, A.P., Taranukha, T., Elghazi, L., Cras-Méneur, C., and Bernal-Mizrachi, E. (2012). MTORC1 signaling and regulation of pancreatic β-cell mass. Cell Cycle *11*, 1892–1902. https://doi.org/10.4161/cc.20036.
23. Rachdi, L., Balcazar, N., Osorio-Duque, F., Elghazi, L., Weiss, A., Gould, A., Chang-Chen, K.J., Gambello, M.J., and Bernal-Mizrachi, E. (2008). Disruption of Tsc2 in pancreatic β cells induces β cell mass expansion and improved glucose tolerance in a TORC1-dependent manner. Proc. Natl. Acad. Sci. USA *105*, 9250–9255. https://doi.org/10.1073/pnas.0803047105.
24. Mori, H., Inoki, K., Opland, D., Münzberg, H., Villanueva, E.C., Faouzi, M., Ikenoue, T., Kwiatkowski, D.J., MacDougald, O.A., Myers, M.G., and Guan, K.L. (2009). Critical roles for the TSC-mTOR pathway in β-cell function. Am. J. Physiol. Endocrinol. Metab. *297*, E1013–E1022. https://doi.org/10.1152/ajpendo.00262.2009.
25. Blandino-Rosano, M., Barbaresso, R., Jimenez-Palomares, M., Bozadjieva, N., Werneck-de-Castro, J.P., Hatanaka, M., Mirmira, R.G., Sonenberg, N., Liu, M., Rüegg, M.A., et al. (2017). Loss of mTORC1 signalling impairs β-cell homeostasis and insulin processing. Nat. Commun. *8*, 16014. https://doi.org/10.1038/ncomms16014.
26. Alejandro, E.U., Bozadjieva, N., Blandino-Rosano, M., Wasan, M.A., Elghazi, L., Vadrevu, S., Satin, L., and Bernal-Mizrachi, E. (2017). Overexpression of kinase-dead mTOR impairs glucose homeostasis by regulating insulin secretion and not β-cell mass. Diabetes *66*, 2150–2162. https://doi.org/10.2337/db16-1349.
27. Asahara, S.I., Inoue, H., Watanabe, H., and Kido, Y. (2022). Roles of mTOR in the Regulation of Pancreatic β-Cell Mass and Insulin Secretion. Biomolecules *12*, 614. https://doi.org/10.3390/BIOM12050614.
28. Sinagoga, K.L., Stone, W.J., Schiesser, J.V., Schweitzer, J.I., Sampson, L., Zheng, Y., and Wells, J.M. (2017). Distinct roles for the mTOR pathway in postnatal morphogenesis, maturation and function of pancreatic islets. Development *144*, 2402–2414. https://doi.org/10.1242/dev.146316.
29. Jaafar, R., Tran, S., Shah, A.N., Sun, G., Valdearcos, M., Marchetti, P., Masini, M., Swisa, A., Giacometti, S., Bernal-Mizrachi, E., et al. (2019).

MTORC1-to-AMPK switching underlies βcell metabolic plasticity during maturation and diabetes. J. Clin. Invest. *129*, 4124–4137. https://doi.org/10.1172/JCI127021.

30. Ni, Q., Gu, Y., Xie, Y., Yin, Q., Zhang, H., Nie, A., Li, W., Wang, Y., Ning, G., Wang, W., and Wang, Q. (2017). Raptor regulates functional maturation of murine beta cells. Nat. Commun. *8*, 15755. https://doi.org/10.1038/ncomms15755.

31. Helman, A., Cangelosi, A.L., Davis, J.C., Pham, Q., Rothman, A., Faust, A. L., Straubhaar, J.R., Sabatini, D.M., and Melton, D.A. (2020). A Nutrient-Sensing Transition at Birth Triggers Glucose-Responsive Insulin Secretion. Cell Metab. *31*, 1004–1016.e5. https://doi.org/10.1016/j.cmet.2020.04.004.

32. Elghazi, L., Blandino-Rosano, M., Alejandro, E., Cras-Méneur, C., and Bernal-Mizrachi, E. (2017). Role of nutrients and mTOR signaling in the regulation of pancreatic progenitors development. Mol. Metab. *6*, 560–573. https://doi.org/10.1016/j.molmet.2017.03.010.

33. Ardestani, A., Lupse, B., Kido, Y., Leibowitz, G., and Maedler, K. (2018). mTORC1 Signaling: A Double-Edged Sword in Diabetic β Cells. Cell Metabolism *27*, 314–331. https://doi.org/10.1016/j.cmet.2017.11.004.

34. Leibowitz, G., Cerasi, E., and Ketzinel-Gilad, M. (2008). The role of mTOR in the adaptation and failure of β-cells in type 2 diabetes. Diabetes Obes. Metab. *10*, 157–169. https://doi.org/10.1111/j.1463-1326.2008.00952.x.

35. Gu, Y., Lindner, J., Kumar, A., Yuan, W., and Magnuson, M.A. (2011). Rictor/mTORC2 is essential for maintaining a balance between β-cell proliferation and cell size. Diabetes *60*, 827–837. https://doi.org/10.2337/db10-1194.

36. Yuan, T., Lupse, B., Maedler, K., and Ardestani, A. (2018). mTORC2 Signaling: A Path for Pancreatic β Cell's Growth and Function. Journal of Molecular Biology *430*, 904–918. https://doi.org/10.1016/j.jmb.2018.02.013.

37. Blandino-Rosano, M., Scheys, J.O., Werneck-De-Castro, J.P., Louzada, R.A., Almaça, J., Leibowitz, G., Rüegg, M.A., Hall, M.N., and Bernal-Mizrachi, E. (2022). Novel roles of mTORC2 in regulation of insulin secretion by actin filament remodeling. Am. J. Physiol. Endocrinol. Metab. *323*, E133–E144. https://doi.org/10.1152/ajpendo.00076.2022.

38. Sinagoga, K.L., Stone, W.J., Schiesser, J.V., Schweitzer, J.I., Sampson, L., Zheng, Y., and Wells, J.M. (2017). Distinct roles for the mTOR pathway in postnatal morphogenesis, maturation and function of pancreatic islets. J. Cell Sci. *130*, e1.1. https://doi.org/10.1242/jcs.207845.

39. Hoenig, M., MacGregor, L.C., and Matschinsky, F.M. (1986). In vitro exhaustion of pancreatic β-cells. Am. J. Physiol. *250*, E502–E511. https://doi.org/10.1152/ajpendo.1986.250.5.e502.

40. Andersson, A. (1978). Isolated mouse pancreatic islets in culture: Effects of serum and different culture media on the insulin production of the islets. Diabetologia *14*, 397–404. https://doi.org/10.1007/BF01228134.

41. Rumala, C.Z., Liu, J., Locasale, J.W., Corkey, B.E., Deeney, J.T., and Rameh, L.E. (2020). Exposure of Pancreatic β-Cells to Excess Glucose Results in Bimodal Activation of mTORC1 and mTOR-Dependent Metabolic Acceleration. iScience *23*, 100858. https://doi.org/10.1016/j.isci.2020.100858.

42. Kaihara, K.A., Dickson, L.M., Jacobson, D.A., Tamarina, N., Roe, M.W., Philipson, L.H., and Wicksteed, B. (2013). β-cell-specific protein kinase A activation enhances the efficiency of glucose control by increasing acute-phase insulin secretion. Diabetes *62*, 1527–1536. https://doi.org/10.2337/db12-1013.

43. Farnsworth, N.L., Walter, R., Piscopio, R.A., Schleicher, W.E., and Benninger, R.K.P. (2019). Exendin-4 overcomes cytokine-induced decreases in gap junction coupling via protein kinase A and Epac2 in mouse and human islets. J. Physiol. *597*, 431–447. https://doi.org/10.1113/JP276106.

44. Xie, J., El Sayed, N.M., Qi, C., Zhao, X., Moore, C.E., and Herbert, T.P. (2014). Exendin-4 stimulates islet cell replication via the IGF1 receptor activation of mTORC1/s6k1. J. Mol. Endocrinol. *53*, 105–115. https://doi.org/10.1530/JME-13-0200.

45. Kwon, G., Marshall, C.A., Pappan, K.L., Remedi, M.S., and McDaniel, M.L. (2004). Signaling elements involved in the metabolic regulation of mTOR by nutrients, incretins, and growth factors in islets. Diabetes *53*, S225–S232. https://doi.org/10.2337/diabetes.53.suppl_3.S225.

46. Ben-Sahra, I., Hoxhaj, G., Ricoult, S.J.H., Asara, J.M., and Manning, B.D. (2016). mTORC1 induces purine synthesis through control of the mitochondrial tetrahydrofolate cycle. Science *351*, 728–733. https://doi.org/10.1126/science.aad0489.

47. Riahi, Y., Kogot-Levin, A., Kadosh, L., Agranovich, B., Malka, A., Assa, M., Piran, R., Avrahami, D., Glaser, B., Gottlieb, E., et al. (2023). Hyperglucagonaemia in diabetes: altered amino acid metabolism triggers mTORC1 activation, which drives glucagon production. Diabetologia *66*, 1925–1942. https://doi.org/10.1007/s00125-023-05967-8.

48. Ravi, V., Jain, A., Mishra, S., and Sundaresan, N.R. (2020). Measuring Protein Synthesis in Cultured Cells and Mouse Tissues Using the Non-radioactive SUnSET Assay. Curr. Protoc. Mol. Biol. *133*, e127. https://doi.org/10.1002/cpmb.127.

49. Gomez, E., Powell, M.L., Greenman, I.C., and Herbert, T.P. (2004). Glucose-stimulated protein synthesis in pancreatic β-cells parallels an increase in the availability of the translational ternary complex (eIF2-GTP-Met-tRNAi) and the dephosphorylation of eIF2α. J. Biol. Chem. *279*, 53937–53946. https://doi.org/10.1074/jbc.M408682200.

50. Reinartz, M., Raupach, A., Kaisers, W., and Gödecke, A. (2014). AKT1 and AKT2 induce distinct phosphorylation patterns in HL-1 cardiac myocytes. J. Proteome Res. *13*. https://doi.org/10.1021/pr500131g.

51. Robitaille, A.M., Christen, S., Shimobayashi, M., Cornu, M., Fava, L.L., Moes, S., Prescianotto-Baschong, C., Sauer, U., Jenoe, P., and Hall, M. N. (2013). Quantitative phosphoproteomics reveal mTORC1 activates de novo pyrimidine synthesis. Science *339*. https://doi.org/10.1126/science.1228771.

52. Demirkan, G., Yu, K., Boylan, J.M., Salomon, A.R., and Gruppuso, P.A. (2011). Phosphoproteomic profiling of in vivo signaling in liver by the mammalian target of rapamycin complex 1 (mTORC1). PLoS One *6*. https://doi.org/10.1371/journal.pone.0021729.

53. Hsu, P.P., Kang, S.A., Rameseder, J., Zhang, Y., Ottina, K.A., Lim, D., Peterson, T.R., Choi, Y., Gray, N.S., Yaffe, M.B., et al. (2011). The mTOR-regulated phosphoproteome reveals a mechanism of mTORC1-mediated inhibition of growth factor signaling. Science *332*. https://doi.org/10.1126/science.1199498.

54. Humphrey, S.J., Yang, G., Yang, P., Fazakerley, D.J., Stöckli, J., Yang, J. Y., and James, D.E. (2013). Dynamic adipocyte phosphoproteome reveals that akt directly regulates mTORC2. Cell Metab. *17*. https://doi.org/10.1016/j.cmet.2013.04.010.

55. Moritz, A., Li, Y., Guo, A., Villén, J., Wang, Y., MacNeill, J., Kornhauser, J., Sprott, K., Zhou, J., Possemato, A., et al. (2010). Akt - RSK - S6 kinase signaling networks activated by oncogenic receptor tyrosine kinases. Sci. Signal *3*. https://doi.org/10.1126/scisignal.2000998.

56. Minard, A.Y., Tan, S.X., Yang, P., Fazakerley, D.J., Domanova, W., Parker, B.L., Humphrey, S.J., Jothi, R., Stöckli, J., and James, D.E. (2016). mTORC1 Is a Major Regulatory Node in the FGF21 Signaling Network in Adipocytes. Cell Rep. *17*. https://doi.org/10.1016/j.celrep.2016.08.086.

57. Yu, Y., Yoon, S.O., Poulogiannis, G., Yang, Q., Ma, X.M., Villén, J., Kubica, N., Hoffman, G.R., Cantley, L.C., Gygi, S.P., et al. (2011). Phosphoproteomic analysis identifies Grb10 as an mTORC1 substrate that negatively regulates insulin signaling. Science *332*. https://doi.org/10.1126/science.1199484.

58. Ståhl, S., Branca, R., Efazat, G., Ruzzene, M., Zhivotovsky, B., Lewensohn, R., Viktorsson, K., and Lehtiö, J. (2011). Phosphoproteomic profiling of NSCLC cells reveals that ephrin B3 regulates pro-survival signaling through Akt1-mediated phosphorylation of the EphA2 receptor. J. Proteome Res. *10*. https://doi.org/10.1021/pr200037u.

59. Liu, L., Luo, Y., Chen, L., Shen, T., Xu, B., Chen, W., Zhou, H., Han, X., and Huang, S. (2010). Rapamycin inhibits cytoskeleton reorganization and cell

motility by suppressing RhoA expression and activity. J. Biol. Chem. *285*, 38362–38373. https://doi.org/10.1074/jbc.M110.141168.

60. Kuleshov, M.V., Jones, M.R., Rouillard, A.D., Fernandez, N.F., Duan, Q., Wang, Z., Koplev, S., Jenkins, S.L., Jagodnik, K.M., Lachmann, A., et al. (2016). Enrichr: a comprehensive gene set enrichment analysis web server 2016 update. Nucleic Acids Res. *44*, W90–W97. https://doi.org/10.1093/nar/gkw377.
61. de Seze, J., Gatin, J., and Coppey, M. (2023). RhoA regulation in space and time. FEBS Lett *597*, 836–849, Preprint. https://doi.org/10.1002/1873-3468.14578.
62. Mosaddeghzadeh, N., and Ahmadian, M.R. (2021). The rho family gtpases: Mechanisms of regulation and signaling. Cells *10*, 1831. https://doi.org/10.3390/cells10071831.
63. Müller, P.M., Rademacher, J., Bagshaw, R.D., Wortmann, C., Barth, C., van Unen, J., Alp, K.M., Giudice, G., Eccles, R.L., Heinrich, L.E., et al. (2020). Systems analysis of RhoGEF and RhoGAP regulatory proteins reveals spatially organized RAC1 signalling from integrin adhesions. Nat Cell Biol *22*. https://doi.org/10.1038/s41556-020-0488-x.
64. Shimokawa, H., Sunamura, S., and Satoh, K. (2016). RhoA/Rho-Kinase in the Cardiovascular System. Circulation research *118*, 352–366. https://doi.org/10.1161/CIRCRESAHA.115.306532.
65. Duan, X., Liu, J., Zhu, C.C., Wang, Q.C., Cui, X.S., Kim, N.H., Xiong, B., and Sun, S.C. (2016). RhoA-mediated MLC2 regulates actin dynamics for cytokinesis in meiosis. Cell Cycle *15*, 471–477. https://doi.org/10.1080/15384101.2015.1128590.
66. Jewell, J.L., Luo, W., Oh, E., Wang, Z., and Thurmond, D.C. (2008). Filamentous actin regulates insulin exocytosis through direct interaction with Syntaxin 4. J. Biol. Chem. *283*, 10716–10726. https://doi.org/10.1074/jbc.M709876200.
67. Kolic, J., Spigelman, A.F., Smith, A.M., Manning Fox, J.E., and MacDonald, P.E. (2014). Insulin secretion induced by glucose-dependent insulinotropic polypeptide requires phosphatidylinositol 3-kinase γ in rodent and human β-cells. J. Biol. Chem. *289*, 32109–32120. https://doi.org/10.1074/jbc.M114.577510.
68. Henquin, J.C., Dufrane, D., Gmyr, V., Kerr-Conte, J., and Nenquin, M. (2017). Pharmacological approach to understanding the control of insulin secretion in human islets. Diabetes Obes. Metab. *19*, 1061–1070. https://doi.org/10.1111/dom.12887.
69. Henquin, J.C., Mourad, N.I., and Nenquin, M. (2012). Disruption and stabilization of β-cell actin microfilaments differently influence insulin secretion triggered by intracellular Ca 2+ mobilization or store-operated Ca 2+ entry. FEBS Lett. *586*, 89–95. https://doi.org/10.1016/j.febslet.2011.11.030.
70. Kong, X., Yan, D., Sun, J., Wu, X., Mulder, H., Hua, X., and Ma, X. (2014). Glucagon-like peptide 1 stimulates insulin secretion via inhibiting RhoA/ROCK signaling and disassembling glucotoxicity-induced stress fibers. Endocrinology (United States) *155*, 4676–4685. https://doi.org/10.1210/en.2014-1314.
71. Bracey, K.M., Ho, K.H., Yampolsky, D., Gu, G., Kaverina, I., and Holmes, W.R. (2020). Microtubules Regulate Localization and Availability of Insulin Granules in Pancreatic Beta Cells. Biophys. J. *118*, 193–206. https://doi.org/10.1016/j.bpj.2019.10.031.
72. Ng, X.W., Chung, Y.H., Asadi, F., Kong, C., Ustione, A., and Piston, D.W. (2022). RhoA as a Signaling Hub Controlling Glucagon Secretion From Pancreatic a-Cells. Diabetes *71*. https://doi.org/10.2337/db21-1010.
73. Cheng, Y., Kim, J., Li, X.X., and Hsueh, A.J. (2015). Promotion of ovarian follicle growth following mTOR activation: Synergistic effects of AKT stimulators. PLoS One *10*, e0117769. https://doi.org/10.1371/journal.pone.0117769.
74. Liu, Z., Zhu, X., Xu, C., Min, F., Yu, G., and Chen, C. (2023). Ulinastatin ameliorates the malignant progression of prostate cancer cells by blocking the RhoA/ROCK/NLRP3 pathway. Drug Dev. Res. *84*, 36–44. https://doi.org/10.1002/ddr.22010.
75. Konstantinova, I., Nikolova, G., Ohara-Imaizumi, M., Meda, P., Kučera, T., Zarbalis, K., Wurst, W., Nagamatsu, S., and Lammert, E. (2007). EphA-Ephrin-A-Mediated β Cell Communication Regulates Insulin Secretion from Pancreatic Islets. Cell *129*, 359–370. https://doi.org/10.1016/j.cell.2007.02.044.
76. Goentoro, L., Shoval, O., Kirschner, M.W., and Alon, U. (2009). The Incoherent Feedforward Loop Can Provide Fold-Change Detection in Gene Regulation. Mol. Cell *36*, 894–899. https://doi.org/10.1016/j.molcel.2009.11.018.
77. Reeves, G.T. (2019). The engineering principles of combining a transcriptional incoherent feedforward loop with negative feedback. J. Biol. Eng. *13*, 62. https://doi.org/10.1186/s13036-019-0190-3.
78. Ben-Sahra, I., and Manning, B.D. (2017). mTORC1 signaling and the metabolic control of cell growth. Current opinion in cell biology *45*, 72–82. https://doi.org/10.1016/j.ceb.2017.02.012.
79. Zhou, X., Clister, T.L., Lowry, P.R., Seldin, M.M., Wong, G.W., and Zhang, J. (2015). Dynamic Visualization of mTORC1 Activity in Living Cells. Cell Rep. *10*, 1767–1777. https://doi.org/10.1016/j.celrep.2015.02.031.
80. Li, R.-J., Xu, J., Fu, C., Zhang, J., Zheng, Y.G., Jia, H., and Liu, J.O. (2016). Regulation of mTORC1 by lysosomal calcium and calmodulin. Elife *5*, e19360. https://doi.org/10.7554/elife.19360.
81. Cooper, D., and Dimri, M. (2022). Biochemistry, Calcium Channels.In: StatPearls [Internet]. StatPearls Publishing. Available from: https://www.ncbi.nlm.nih.gov/books/NBK562198/.
82. Ni, Q., Song, J., Wang, Y., Sun, J., Xie, J., Zhang, J., Ning, G., Wang, W., and Wang, Q. (2021). Proper mTORC1 Activity Is Required for Glucose Sensing and Early Adaptation in Human Pancreatic β Cells. J. Clin. Endocrinol. Metab. *106*, e562–e572. https://doi.org/10.1210/clinem/dgaa786.
83. Goul, C., Peruzzo, R., and Zoncu, R. (2023). The molecular basis of nutrient sensing and signalling by mTORC1 in metabolism regulation and disease. Nature Reviews Molecular Cell Biology *24*, 857–875. https://doi.org/10.1038/s41580-023-00641-8.
84. Yuan, T., Rafizadeh, S., Gorrepati, K.D.D., Lupse, B., Oberholzer, J., Maedler, K., and Ardestani, A. (2017). Reciprocal regulation of mTOR complexes in pancreatic islets from humans with type 2 diabetes. Diabetologia *60*, 668–678. https://doi.org/10.1007/s00125-016-4188-9.
85. Molakandov, K., Berti, D.A., Beck, A., Elhanani, O., Walker, M.D., Soen, Y., Yavriyants, K., Zimerman, M., Volman, E., Toledo, I., et al. (2021). Selection for CD26− and CD49A+ Cells From Pluripotent Stem Cells-Derived Islet-Like Clusters Improves Therapeutic Activity in Diabetic Mice. Front. Endocrinol. *12*, 635405. https://doi.org/10.3389/fendo.2021.635405.

STAR★METHODS

KEY RESOURCES TABLE

REAGENT or RESOURCE	SOURCE	IDENTIFIER
Antibodies		
Guinea Pig anti-insulin Primary	Agilent	Cat# IR002, RRID:AB_2800361
Mouse anti-glucagon	Santa Cruz Biotechnology	Cat# sc-514592; RRID:AB_2904166
Rabbit anti-phospho-S6 ribosomal protein (Ser240/244)	Cell Signaling Technology	Cat# 5364; RRID:AB_10694233
Rat anti-puromycin Antibody, clone 17H1	Sigma-Aldrich	Cat# MABE341, RRID:AB_3677409
Rabbit phospho-Myosin Light Chain 2 (Ser19) Antibody	Cell Signaling Technology	Cat# 3671, RRID:AB_330248
Rabbit phospho-4E-BP1 (Thr37/46) (236B4) Rabbit mAb	Cell Signaling Technology	Cat# 2855; RRID:AB_560835
Mouse anti-F-actin antibody [NH3]	Abcam	Cat# ab205; RRID:AB_302794
Phalloidin-iFluor 594	Abcam	Cat# ab176757; RRID: AB_3695680
Phospho-Akt (Ser473) (D9E) XP® Rabbit mAb	Cell Signaling Technology	Cat# 4060, RRID:AB_2315049
Phospho-AMPKα (Thr172) (40H9) Rabbit mAb	Cell Signaling Technology	Cat# 2535, RRID:AB_331250
Purified Mouse Anti-E-Cadherin	BD Biosciences	Cat# 610181, RRID:AB_397580
Biological samples		
Cadaveric human islets	Prodo labs	N/A
SC-islets	Kadimastem	N/A
Chemicals, peptides, and recombinant proteins		
RPMI 1640 Medium Modified w/o L-Glutamine, w/o Amino acids, Glucose	MyBioSource	MBS652918
RPMI 1640 Medium without Glucose and L-Glutamine	Sartorius	01-101-1A
RPMI 1640 Medium without L-Glutamine	Sartorius	01-104-1A
Collagenase P	Sigma	11213865001
Histopaque®-1077	Sigma	10771
Histopaque®-1119	Sigma	11191
HEPES buffer 1M	Biological industries	03-025-1B
Glutamine 200mM	Biological industries	03-020-1A
D (+)-Glucose	Roth	50-99-7
Accutase	Sigma	A7089
Fetal bovine serum (FBS)	Sigma	F0926
Bovine serum albumin (BSA)	Sigma	A7906
BD Cytofix/Cytoperm™ Kit	BD Biosciences	554714
Insulin	Sigma	I2643
S961	Novonordisk	N/A
Forskolin	TCI	F0855
Diazoxide	Sigma	D9035
Exendin-4	APExBIO	A3408
Nifedipine	Sigma	N7634
Tolbutamide	Sigma	T0891
KCl	BioLab	001638059100
GKA	Pfizer	HY-108328
Torin-1	EMD millipore	475991

(*Continued on next page*)

Continued		
REAGENT or RESOURCE	SOURCE	IDENTIFIER
Rapamycin	Sigma	37094
Cycloheximide	Mercury	239763
Latrunculin A	Sigma	L5163
Rhosin	Merck	1173671-63-0
Rho Activator II CN03	Cytoskeleton	CN03-B
Recombinant Human Ephrin-A5 Fc	R&D systems	374-EA-200
ML 7 hydrochloride	R&D systems	4310
MHY1485	MCE	HY-B0795
Critical commercial assays		
Human Insulin ELISA	Mercodia	10-1113-01
Ultra-Sensitive Rat Insulin ELISA Kit	Crystal chem	90060
flow cytometry tubes	BD Falcon	352235
G-Actin/F-actin *In Vivo* Assay Biochem Kit	Cytoskeleton	BK037
Deposited data		
Phosphoproteomic raw data	PRIDE	PXD062389
Experimental models: Organisms/strains		
C57BL/6	Jackson Laboratory	N/A
Software and algorithms		
Prism (version 9)	GraphPad	https://www.graphpad.com/features
FlowJo (version 10)	N/A	https://www.flowjo.com/flowjo/download
ImageJ (version 1.9.22)	N/A	https://imagej.net/ij/

EXPERIMENTAL MODEL AND STUDY PARTICIPANT DETAILS

Mice

C57BL/6 mice were used for islet isolation for GSIS and FACS analysis, and immunohistochemistry. 8- to 12-week-old male C57BL/6 mice were obtained from Harlan, Israel. For the *in vivo* glucose-stimulated insulin secretion assays, mice were fasted for 14 h. Diazoxide (40mg/kg_{bw})/forskolin (20mg/kg_{bw})/Torin-1 (20mg/kg_{bw}) were injected into the intraperitoneal space, followed by 20% glucose intraperitoneal injection (2g/kg_{bw}). Blood was collected at two time points, right before the start of the injections, and after the glucose injection. We separated the serum from the whole blood content by 20 min of centrifugation at 4°C, 10,000g. Insulin was quantified by an enzyme-linked immunosorbent assay (ELISA) (Crystal Chem). The joint Institutional Animal Care and Use Committee of the Hebrew University approved the study protocol for animal welfare. The Hebrew University is accredited by the Association for Assessment and Accreditation of Laboratory Animal Care International.

Human islets

We used live human islets for phospho-proteomics profiling, FACS, and GSIS analysis from the pancreata of a brain-dead subject obtained from Prodo labs (HP-24064-02 and HP-24327-01) and from the University of Pennsylvania Islet Transplant Center (SAMN41393792 and SAMN47319182). Technical replicates were used in the relevant experiments.

Human SC-islets

Fully differentiated SC-islets were generated by Kadimastem as previously described.[85] Highly pluripotent, clinical grade, human ES cells HADC-100 were grown to confluent monolayers in essential E8 medium (Gibco), with the addition of penicillin and streptomycin (PS, Gibco) on vitronectin-coated flasks (Gibco). Differentiation was performed on cell aggregates formed in spinner flasks for 2 days in dynamic suspension cultures. In brief, 48 h before starting the differentiation protocol (day 2), non-differentiated cells were dissociated with Versene (Gibco). Single cells washed with $PBS^{-/-}$ (Gibco), were seeded in 500 mL disposable spinner flasks (Corning), filled with 250 mL E8 medium containing 10 μM Rock Inhibitor Y27632 (Cayman Chemical), at a concentration of 0.8–1 × 106 cells/ml. The spinner flasks were placed on a magnetic stirrer (DURA-MAG, 9 position stirrer, Chemglass) at a speed of 70 rpm in a humidified incubator set at 5% CO2 and 37°C. This resulted in the formation of ES cell clusters in suspension, as well as in cell proliferation. On day −1, 80% of the E8 medium was replaced. On Day 0, the E8 medium was washed away by letting the aggregates settle for 5 min and removing the supernatant with a pipette. Cells were washed with 250 mL $PBS^{-/-}$; after 3 min stirring in the incubator, $PBS^{-/-}$ was replaced by 250 mL of stage 1 differentiation medium. The media for the seven-stage differentiation protocol was refined based on several published protocols.

METHOD DETAILS

Ex vivo GSIS and FACS assays

We isolated islets from a whole pancreas using collagenase P (Roche) injected into the bile duct, followed by isolation on a Histopaque gradient (Sigma). Islets from different mice were pooled into biological replicates and incubated overnight in an RPMI-1640 medium supplemented with 10% FBS, l-glutamine, and penicillin-streptomycin in a 37°C, 5% CO2 incubator. Each mouse islets were placed in basal Krebs buffer (KRB) (119 mM NaCl, 4.6 mM KCl, 2 mM CaCl2, 1 mM MgCl2, 0.15 mM Na2HPO4, 0.4 mM KH2PO4, 5 mM NaHCO3, 20 mM HEPES, 0.05% BSA) supplemented with 2.8mM glucose or into a nutrient-free RPMI-1640 medium (MyBioSource, MBS652918) supplemented with 2.8mM glucose and 0.02% BSA, with no amino acids or serum, for 30 min of incubation. Then, 25–30 islets were handpicked for each assay replicate and were incubated for 45 min in KRB or RPMI-1640 with low (2.8 mM) or high (16.7 mM) glucose concentrations, in 6-well plates at 37°C, 5% CO_2. The following compounds were used: insulin (Sigma, 100 nM), S961 (Novonordisk, 1 μM), forskolin (TCI, 10 nM), diazoxide (Sigma, 250 μM), KCl (BioLab, 30 mM), GKA (Pfizer, 10 μM), exendin-4 (APExBIO, 100 nM), nifedipine (Sigma, 10 μM), tolbutamide (Sigma, 100 μM), Torin-1 (EMD Millipore, 100 nM), rapamycin (Sigma, 100 nM), cycloheximide (Mercury, 50ug/ml), latrunculinA (Sigma, 0.5 μg/ml), rhosin (Merck, 100 μM), CN03 (Cytoskeleton, 1 μg/mL), ephrin-A5 FC (R&D systems, 4 μg/mL), ML-7 (R&D systems, 5 μM), MHY1485 (MCE, 10μM). After 45 min of incubation, the medium was collected. We measured the insulin concentrations by an Ultrasensitive Insulin ELISA kit (Crystal Chem). For FACS staining, we collected the islets into 1.7 mL Eppendorf tubes and dispersed them into a single-cell suspension by 5-min incubation in Accutase (Sigma) at 37°C until clusters dissociated to single cells upon mixing by pipetting gently up and down. Cells were centrifuged for 1 min at 1000 rpm, resuspended in a cytofix/cytoperm (BD Biosciences) solution, and incubated for 20 min. Cells were then washed once in perm/wash (BD Biosciences), resuspended in perm/wash with primary antibodies, and incubated at room temperature for 1 h. Primary antibodies were diluted as noted: guiana-pig anti-insulin (Agilent IR002; 1:5), rabbit anti-phospho-S6 ribosomal protein (Ser240/244) (Cell Signaling 5364; 1:300), rabbit anti-phospho-4E-BP1 (Thr37/46) (236B4) (Cell Signaling 2855; 1:200), rabbit anti phospho-Akt (Ser473) (Cell Signaling 4060; 1:200), rabbit anti phospho-AMPKα (Thr172) (40H9) (Cell Signaling 2535; 1:200), rat anti-puromycin (clone 17H1) (Sigma-Aldrich MABE341; 1:300), mouse anti-F-actin [NH3] (Abcam ab205; 1:100), phalloidin-iFluor 594 (Abcam ab176757; 1:2000). Cells were washed once in a perm/wash buffer and then incubated in a perm/wash buffer with secondary antibodies for 45 min. Secondary antibodies conjugated to Alexa Fluor 488, Cy5, Cy3, or 594, were used to visualize primary antibodies. Cells were then washed in a perm/wash solution, resuspended in 150μL perm/wash, filtered through a 40mm nylon mash into flow cytometry tubes, and analyzed using the flow cytometer. Analysis of the results was performed using FlowJo software.

Immunohistochemistry

For the immunohistochemistry assays, mice were fasted overnight and then received Diazoxide (40 mg/kg kg_{bw}), Forskolin, or Torin-1 (20mg/kg_{bw}) by intraperitoneal injection, followed by 20% glucose intraperitoneal injection (20mg/kg_{bw}). Afterward, the pancreas was harvested and placed in a 4% PFA solution for a 4-h incubation at room temperature. The pancreas was then transferred into a 4% PFA solution containing 30% sucrose for overnight incubation at 4°C, then blocked into OCT/Paraffin blocks. Isolated islets were produced and incubated in the conditions described in the previous section. Sliced pancreas tissue or isolated islets were stained for insulin, phospho-S6, and actin filaments using the following primary antibodies: guinea pig anti-insulin (Agilent IR002; 1:20), rabbit anti-phospho-S6 Ribosomal Protein (Ser240/244) (Cell Signaling; 5364L; 1:300), mouse anti-e-cadherin (BD Biosciences, 61018; 1:300), and phalloidin-iFluor 594 conjugate (Abcam ab176757; 1:1000). Secondary antibodies conjugated to Alexa Fluor 488, and Cy5 were used to visualize primary antibodies. The slides were mounted in a mounting medium (Invitrogen Fluoromount-G) and covered with coverslips. Images were taken using Leica Stellaris 5 FLIM STED confocal microscope. Using ImageJ version 1.54f, each islet was manually marked to quantify the intensities of F-actin, and pS6. Visual representations of the Z-stacks images were utilized using Imaris version 10.0.1. The movies were captured as mp4 and available as supporting information.

Ex vivo dynamic glucose stimulated insulin secretion (GSIS)

30-40 islets were divided into chambers and assayed on a fully automated Perifusion System (BioRep). Chambers were sequentially perfused with 2.8 mM with or without Torin-1 (100 nM), 16.7 mM glucose with or without Torin-1 (100 nM) and 2.8 mM glucose with 30 mM KCl in KRB buffer or RPMI-1640 at a flow rate of 100ul/min. Chambers were first perifused with low glucose (2.8 mM) for 16 min for low glucose incubation. The samples were then perifused with high glucose (16.7 mM) for 32 min, low glucose for 16 min, and 30 mM KCl for 16 min. Torin-1 (100 nM) was administered during the first low glucose phase and throughout the high glucose incubation. Insulin concentrations in the supernatant were measured using an Ultrasensitive Insulin ELISA kit. (Crystal chem).

Phospho-proteomics

For each technical replicate, approximately 800 human islets or 1 × 106 SC-islet cells were pre-incubated in basal RPMI-1640 medium for 30 min. The islets were then transferred to a high-glucose medium, with or without 100 nM Torin-1, for 45 min. After incubation, the islets were collected into 1.7 mL Eppendorf tubes and washed three times with ice-cold PBS. The samples were subjected to tryptic digestion using an S-trap. The resulting peptides were enriched for phospho-peptides on IMAC cartridges with a Bravo automated liquid handling system and then further analyzed using nanoflow liquid chromatography (nanoAcquity) coupled to high resolution, high mass accuracy mass spectrometry (Q Exactive HF). Each sample was analyzed on the instrument separately in a

random order in discovery mode. Raw data was processed with MetaMorpheus v1.0.2. The data was searched against the human Uniprot proteome database appended with a list of common lab protein contaminants. Quantification was performed using the embedded FlashLFQ and protein inference algorithms. The processing included the unique G-PTM-D method for identifying dozens of PTMs. The phospho intensities were calculated and used for generating the phospho sites intensities with an in-house script. The output was introduced into Perseus v1.6.2.3 for further analysis. The intensities were log-transformed and only sites with at least two valid values in at least one experimental group were kept. The remaining missing values were imputed using a low value (1024). A student's t-test was used to detect differentially expressed sites between the groups. Pathway enrichment analysis of the significant hits was performed using Enrichr (https://maayanlab.cloud/Enrichr).

Primary hepatocytes

primary hepatocytes were isolated from 8- to 12-week-old male C57BL/6 mice by perfusion with liver digest medium (Invitrogen, 17703-034) followed by 70 μm mesh filtration. Percoll (Sigma, P7828) gradient centrifugation allowed primary hepatocytes isolation from other cell types and debris. Cells were seeded in plating medium (DMEM with 10% FBS, 2 mM sodium pyruvate, 1% penicillin/streptomycin, 1 μM dexamethasone, and 100nM insulin). After 4 h of seeding, the medium was changed and incubated overnight in maintenance medium (DMEM, 0.2% BSA, 2mM sodium pyruvate, 1% penicillin/streptomycin, 0.1 μM dexamethasone, and 1nM insulin). Cells were treated and collected within 24h after isolation.

Puromycin labeling

Mouse islets and primary hepatocytes were incubated for 30 min in basal RPMI-1640, followed by 45 min incubation in the following different treatments: low glucose (2.8 mM), high glucose (16.7 mM), insulin (100 nM), Torin-1 (100 nM), and cycloheximide (50 μg/ml). During the final 30 min, the cells were supplemented with 10 μg/mL of puromycin. We collected the cells, dissociated them, and fixed them as described in the FACS assays section.

Measurement of G-actin and F-actin ratio

G-actin and F-actin levels were measured using the G-actin/F-actin *In Vivo* Assay Kit (Cytoskeleton, Cat. # BK037). A total of 400 islets were first incubated in nutrient-free basal media for 30 min, followed by a 45-min incubation in 16.7 mM glucose with or without 100nM Torin-1. The islets were then lysed in LAS2 buffer, homogenized, and incubated at 37°C for 10 min. Unbroken cells and tissue debris were removed by centrifugation at 350*g* for 5 min. The supernatant was then centrifuged at 100,000g for 1 h to separate F-actin (pellet) from G-actin (supernatant). The pellet was resuspended in F-actin depolymerization buffer and incubated on ice for 1 h. Both soluble and insoluble fractions were mixed with SDS sample buffer and analyzed by SDS-PAGE (4–15% polyacrylamide gel), followed by western blotting on a PVDF membrane. Actin was detected using an anti-actin mouse monoclonal antibody and visualized via chemiluminescence. Semi-quantification of western blot signals was performed using Image Lab software.

Calcium imaging

Pancreatic islets were isolated and partially dissociated using Accutase. The islets were then plated in a 96-well plate pre-coated with 1% penicillin/streptomycin, 1% ECM, and 0.5% fibronectin in high-glucose DMEM. Islets were infected with AAV. KP1-CAG-GCamP8m for 24 h, followed by washing and an additional 48-h culture period. Before imaging, the islets were washed and incubated in nutrient-free basal media for 30 min. They were then exposed to 20mM glucose with or without 100nM Torin-1 for 10 min, followed by the addition of 30 mM KCl in low-glucose buffer for 2 min to induce cell depolarization. Throughout imaging, the islets were maintained at 37°C with 5% CO_2. High-resolution time-series images were acquired using an Andor Benchtop Confocal BC43 microscope. A total of 1,800 images were captured over the 10-min glucose challenge (one every 20 ms), followed by an additional 2 min of imaging after KCl addition. The images were stacked, converted into an AVI-format movie, and analyzed using ImageJ/Fiji imaging software with the ROI Manager tool.

QUANTIFICATION AND STATISTICAL ANALYSIS

All conditions in all of the described experiments were performed in three biological replicates or more. For mouse islet experiments, a biological replicate is defined as islets pooled from multiple mice. Each data point represents a biological replicate and error bars represent the standard error of biological replicates. In the immunohistochemistry assays, each dot represents the mean intensity of at least 4 sections, containing a total of at least 10 islets per mouse. In pairwise comparisons, statistical significance was determined by a two-tailed, unpaired t test. In multiple comparisons, statistical significance was determined by ordinary one-way ANOVA, or the Brown-Forsythe and Welch ANOVA tests when treatments resulted in unequal standard deviations (comparisons were made between all conditions, only statistically significant comparisons are depicted in most cases). One asterisk denotes the statistical significance of p-value ≤ 0.05. Two asterisks denote the statistical significance of p-value ≤ 0.01. Three asterisks denote statistical significance of p-value ≤ 0.001. Four asterisks denote statistical significance of p value ≤ 0.001. 'ns' denotes the statistical significance of p value ≥ 0.05. Data were analyzed and plotted using Prism software from GraphPad.